

Master's Degree in Energy and Nuclear  
Engineering

# Complex Energy Systems Optimization

Via Rolling Horizon algorithm

Master's Degree Thesis



**Author**

Stefano Caldarone

**Supervisors**

Vittorio Verda

Elisa Guelpa

Martina Capone

Department of Energy

Politecnico di Torino

A.A 2019/2020



# Abstract

The objective of this thesis is the optimal operation of a complex energy system via the “Rolling Horizon” algorithm (also known as “Receding Horizon” or “Model Predictive Control”). The target of the optimization will be achieving the lowest possible monetary expense given a pre-determined energy demand (heating, cooling and electric power), by determining the optimal mix of power production from the components of a HRES system, including the option of buying or selling energy to the national grid. The energy system will also be subjected to uncertainty in the energy demand forecast, which is going to be managed thanks to the Rolling Horizon algorithm. The computation will be carried out using *MATLAB*.

After an overview of the Rolling Horizon algorithm, its implementation for this thesis’ purposes will be examined in a step-by-step fashion. Afterwards, the results obtained will be presented, and a sensitivity analysis on the most relevant parameters will be performed. In the end, the necessary conclusions will be drawn.



# Contents

<b>1</b>	<b>Introduction</b>	<b>13</b>
<b>2</b>	<b>Case Study</b>	<b>15</b>
2.1	Presentation of the problem . . . . .	15
2.2	Description of the system's components . . . . .	16
2.2.1	Combined Heat and Power . . . . .	16
2.2.2	Gas Heat Pump . . . . .	17
2.2.3	Boiler . . . . .	18
2.2.4	Absorption Chiller . . . . .	18
2.2.5	Electric Chiller . . . . .	19
2.2.6	Storage . . . . .	19
2.2.7	Photovoltaic . . . . .	20
2.2.8	Wind Turbine . . . . .	21
2.2.9	Summary . . . . .	22
<b>3</b>	<b>The Rolling Horizon method</b>	<b>23</b>
3.1	Background . . . . .	23
3.2	Peculiarities of the method . . . . .	23
3.3	Algorithm overview . . . . .	24
3.3.1	Time discretization . . . . .	24
3.3.2	Prediction Horizon and Control Horizon . . . . .	24
3.3.3	System modelization . . . . .	25
3.3.4	Optimization Problem . . . . .	26
3.3.5	Application of the algorithm and re-iteration . . . . .	27
3.4	Application of the algorithm in the case study . . . . .	28
3.4.1	Time discretization . . . . .	28
3.4.2	Prediction and Control Horizon . . . . .	28
3.4.3	Uncertainty . . . . .	28
3.4.4	Flow diagram of the algorithm . . . . .	29
<b>4</b>	<b>Optimization problem formulation</b>	<b>31</b>
4.1	Efficiency curves linearization . . . . .	31
4.2	Implementation of linear optimization . . . . .	32
4.2.1	Control variables . . . . .	32
4.2.2	Objective function . . . . .	33
4.2.3	Linear constraints . . . . .	33
4.3	Issues with linear optimization . . . . .	35
4.3.1	Efficiency's zero-degree term . . . . .	35
4.3.2	Minimum value of variables . . . . .	35

4.3.3	Inaccurate linear efficiency . . . . .	35
4.4	Implementation of MILP optimization . . . . .	35
4.4.1	Definition of the binary variables . . . . .	36
4.4.2	Additional constraints . . . . .	36
4.4.3	Piecewise linearization of efficiency curves . . . . .	36
4.4.4	Inequality constraints . . . . .	38
4.4.5	Equality constraints . . . . .	40
4.4.6	Implementation in MATLAB . . . . .	41
<b>5</b>	<b>Optimization results</b>	<b>43</b>
5.1	Results of the optimization . . . . .	44
5.1.1	Heating . . . . .	44
5.1.2	Cooling . . . . .	45
5.1.3	Electricity . . . . .	46
5.1.4	Storage . . . . .	47
5.2	Considerations . . . . .	47
5.3	Assessment of the algorithm's effectiveness . . . . .	48
5.3.1	Comparison with standard MILP optimization . . . . .	49
5.4	Error due to linearization . . . . .	51
<b>6</b>	<b>Sensitivity analyses results</b>	<b>53</b>
6.1	Sensitivity analysis on the Prediction Horizon . . . . .	53
6.2	Sensitivity analysis on selling/buying price ratio . . . . .	54
6.3	Error due to linearization . . . . .	54
6.4	Uncertainty generation . . . . .	56
6.5	Imposed value of storage . . . . .	59
6.5.1	Imposed value on all three storage units . . . . .	60
6.5.2	Imposed value on heat storage . . . . .	61
6.5.3	Imposed value on cool storage . . . . .	62
6.5.4	Imposed value on electric storage . . . . .	63
6.6	Initial level of storage . . . . .	64
<b>7</b>	<b>Conclusions</b>	<b>67</b>





# List of Figures

2.1	A CHP unit. . . . .	16
2.2	Efficiency curves of the CHP system. . . . .	16
2.3	Schematization of a GHP system. . . . .	17
2.4	Efficiency curves of the GHP system. . . . .	17
2.5	A gas boiler. . . . .	18
2.6	Heating efficiency curve of the boiler. . . . .	18
2.7	An absorption chiller. . . . .	18
2.8	Cooling efficiency of the absorption chiller. . . . .	18
2.9	An electric chiller. . . . .	19
2.10	Cooling efficiency of the electric chiller. . . . .	19
2.11	Storage units. . . . .	19
2.12	A monocrystalline silicon PV panel. . . . .	20
2.13	PV efficiency compared to environment's temperature. . . . .	20
2.14	A wind turbine. . . . .	21
2.15	Wind power values generation method. . . . .	21
3.1	Representation of the vehicle problem. . . . .	24
3.2	Prediction Horizon. . . . .	25
3.3	Implementation of Rolling Horizon . . . . .	26
3.4	Schematization of the Rolling Horizon algorithm. . . . .	27
3.5	Flow diagram of the MATLAB algorithm. . . . .	29
4.1	Efficiency curves linearization. . . . .	32
4.2	Comparison between one-piece and three-piece linear fit of the chiller's efficiency . . . . .	37
4.3	Comparison between one-piece and two-piece linear fit of the gas heat pump's cooling efficiency . . . . .	37
5.1	Results for heating power . . . . .	44
5.2	Results for cooling power. . . . .	45
5.3	Results for electric power. . . . .	46
5.4	Energy cumulated in the heating, cooling and electric storages. . . . .	47
5.5	Results of the priority order simulation. . . . .	49
5.6	Results of the standard MILP optimization. . . . .	50
6.1	Sensitivity analysis on the parameter $PH$ . . . . .	53
6.2	Sensitivity analysis on the parameter $k$ . . . . .	54
6.3	Energy sold for each value of the parameter $k$ . . . . .	55
6.4	Relative error due to linearization. . . . .	55
6.5	Absolute error due to linearization. . . . .	56

6.6	Uncertainty generation for heating demand. . . . .	57
6.7	Uncertainty generation for cooling demand. . . . .	57
6.8	Uncertainty generation for electricity demand. . . . .	58
6.9	Sensitivity analysis for the constant uncertainty generation method. . . . .	58
6.10	Sensitivity analysis for the uncertainty depending on peaks generation method. . . . .	59
6.11	Imposed level on 3 storage units: constant uncertainty . . . . .	60
6.12	Imposed level on 3 storage units: uncertainty depending on peaks . . . . .	60
6.13	Difference between minimum and maximum objective function value. . . . .	60
6.14	Imposed level on heat storage: constant uncertainty . . . . .	61
6.15	Imposed level on heat storage: uncertainty depending on peaks . . . . .	61
6.16	Difference between minimum and maximum objective function value. . . . .	61
6.17	Imposed level on cool storage: constant uncertainty . . . . .	62
6.18	Imposed level on cool storage: uncertainty depending on peaks . . . . .	62
6.19	Difference between minimum and maximum objective function value. . . . .	62
6.20	Imposed level on electric storage: constant uncertainty . . . . .	63
6.21	Imposed level on electric storage: uncertainty depending on peaks . . . . .	63
6.22	Difference between minimum and maximum objective function value. . . . .	63
6.23	Sensitivity of the objective function to the storage's initial level. . . . .	65





# Chapter 1

## Introduction

The ever-increasing energy demand (according to IEA's *Current Policies* scenario, energy demand will rise by 1.3% each year to 2040, with increasing demand for energy services unrestrained by further efforts to improve efficiency<sup>1</sup>), the greenhouse-gas emissions regulations and the limited availability of fossil fuel reserves have led many power producers to shift towards renewable energy, the fastest-growing of which are solar and wind power. However, such energy sources depend heavily on weather and climatic conditions and present severe fluctuations in power generation.

This is why energy source diversification has become of utmost importance: mixes of two or more sources coupled with a suitable storage system (also known as Hybrid Renewable Energy Systems or HRES) have proven to be a valid and reliable power generation method. In order to better exploit the several technologies these systems are composed of, the control and operation of HRES is often performed with the aid of optimization algorithms. To this end, it is necessary to have some form of forecast of the future energy demand (the more accurate the prediction, the more efficient the optimization), which is going to be used by the algorithm to achieve the most efficient system configuration that satisfies that demand.

A few examples<sup>2</sup> of the most widely used optimization algorithms in the energy field are:

- **Genetic Algorithms:** developed by John Holland and later popularized by Goldberg, it is a family of algorithms which emulates the population and natural genetics mechanisms present in nature; this type of algorithm is very useful to avoid the problem of being "stuck" on local minima.
- **Particle Swarm Optimization:** developed by Kennedy and Eberhart, it emulates the swarm intelligence behavior of birds and fishes. The advantages of this algorithm are its simplicity of implementing, relative flexibility, low memory requirements and short convergence times.
- **Fuzzy Logic Control:** developed by L. Zadeh, it performs the comparison of a set of multiple logical states (differently from binary logic, in which a statement can be either true (1) or false (0)). Fuzzy logic is advantageous for implementing optimal control as a number of input parameters can be taken into the design of the fuzzy rule base to achieve the desired control objective.

---

<sup>1</sup>IEA. *World Energy Outlook 2019*. 2019.

<sup>2</sup>Barnam Saharia. "A review of algorithms for control and optimization for energy management of hybrid renewable energy systems". In: *Journal of Renewable and Sustainable Energy* (2018).

- **Rolling Horizon:** developed independently by Richalet *et al.* (1978) and Cutler and Ramaker (1980),<sup>3</sup> it operates by dividing the problem at hand in smaller sub-problems, whose scope is a smaller time window than that of the original one. It is very useful when the future forecast is characterized by uncertainty and there's a need to update input data with the passing of time.

In the following chapters of this work, the Rolling Horizon algorithm will be further analyzed and implemented in the operation of a HRES system.

---

<sup>3</sup>Giovani Cavalcanti Nunes. *Design and analysis of multivariable predictive control applied to an oil-water-gas separator: a polynomial approach*. 2001. URL: <http://citeseerx.ist.psu.edu/viewdoc/download?doi=10.1.1.6.6300&rep=rep1&type=pdf>.

# Chapter 2

## Case Study

### 2.1 Presentation of the problem

The case that is going to be analyzed in this thesis will involve the optimization of the operation of a Hybrid Renewable Energy System. The system is connected to the electric grid and the district heating grid, with the option of both buying and selling electric and thermal power to them. Furthermore, the system is able to purchase natural gas from the national distribution system. The time period over which the optimization is going to be performed is 24 hours, while the chosen  $\Delta t$  for the discretization of the problem will be 15 minutes. The following data are provided beforehand:

- The system's energy demand in terms of heating, cooling and electricity (respectively  $\Phi_H, \Phi_C, \Phi_E$ ) over the 24 hours; note that these values are merely a forecast, thus being subjected to uncertainty
- The components' minimum and maximum generated power and their efficiency curves
- The storage systems' capacity
- The electric power produced by the photovoltaic panels ( $\Phi_{PV}$ ) during the course of the day
- The maximum electric power which the wind turbine is able to produce ( $\Phi_{wind,max}$ )
- The cost of electricity during the day ( $c_E$ )
- The average cost of thermal power for district heating ( $c_H$ )
- The average cost of natural gas ( $c_G$ )

## 2.2 Description of the system's components

### 2.2.1 Combined Heat and Power

A Combined Heat and Power unit (Figure 2.1) is a system capable of producing electricity by exploiting the enthalpy of a gas (usually air) which is heated via fuel combustion (in this case the fuel is natural gas) and sent into a turbine which converts the gas' internal energy first into mechanical and then electric power via an alternator. The gas exits the turbine at 400-600°C: its remaining thermal energy is then available for consumption. To summarize, the CHP system is able to produce both electric power ( $\Phi_{CHP,E}$ ) and heat ( $\Phi_{CHP,H}$ ) via the combustion of a natural gas mass flow at the inlet ( $\Phi_{CHP,G}$ ). The component's efficiency curves are shown in Figure 2.2.

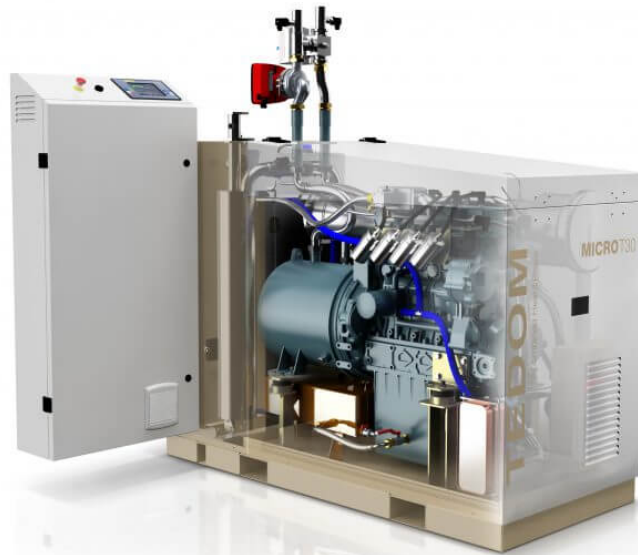


Figure 2.1: A CHP unit.<sup>1</sup>

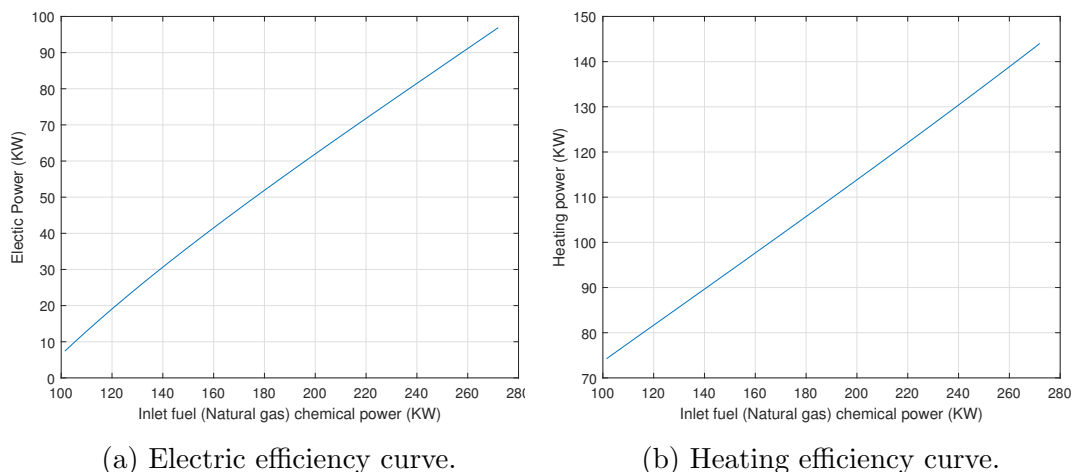


Figure 2.2: Efficiency curves of the CHP system.

## 2.2.2 Gas Heat Pump

The Gas Heat Pump (Figure 2.3) is able to produce both cooling ( $\Phi_{GHP,E}$ ) and heating ( $\Phi_{GHP,H}$ ) thermal power via the combustion of a natural gas mass flow, which is used to supply a thermodynamic cycle ( $\Phi_{GHP,G}$ ). The component's efficiency curves are shown in Figure 2.4.

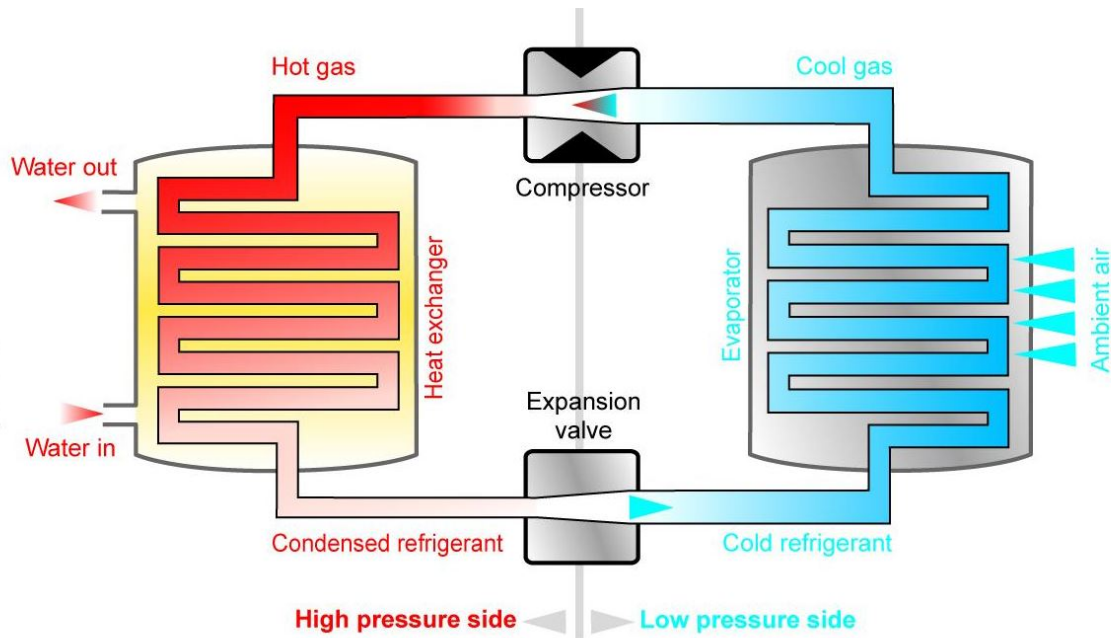


Figure 2.3: Schematization of a GHP system.<sup>2</sup>

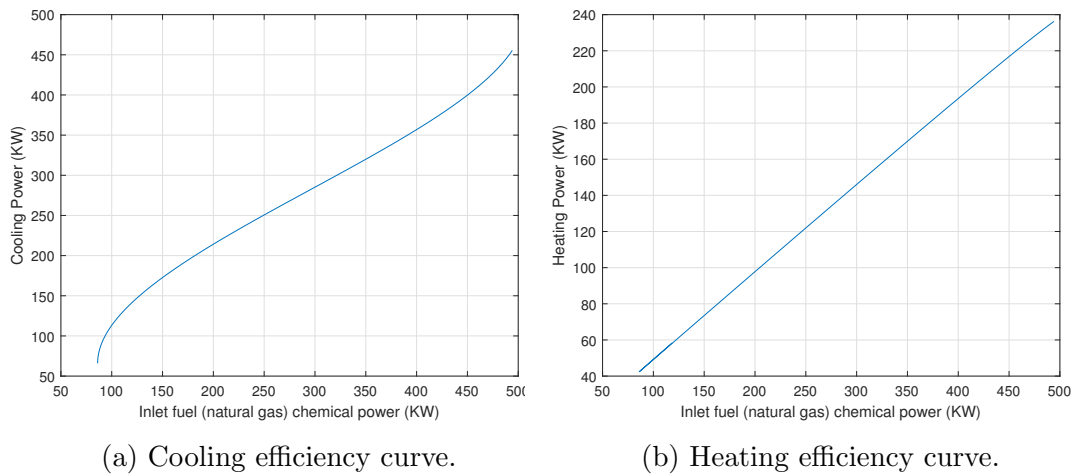


Figure 2.4: Efficiency curves of the GHP system.

<sup>1</sup>TEDOM a.s. URL: <https://www.tedom.com>

<sup>2</sup>Efficient energy centre. URL: <http://www.efficientenergycentre.co.uk/heat-pumps/>

### 2.2.3 Boiler

The boiler (Figure 2.5) exploits the combustion of a natural gas mass flow ( $\Phi_{Boil,G}$ ) to heat ( $\Phi_{Boil,H}$ ) a water flow. In this case, the efficiency will be considered constant and equal to 0.9, so the efficiency curve (Figure 2.6) is a straight line.



Figure 2.5: A gas boiler.<sup>3</sup>

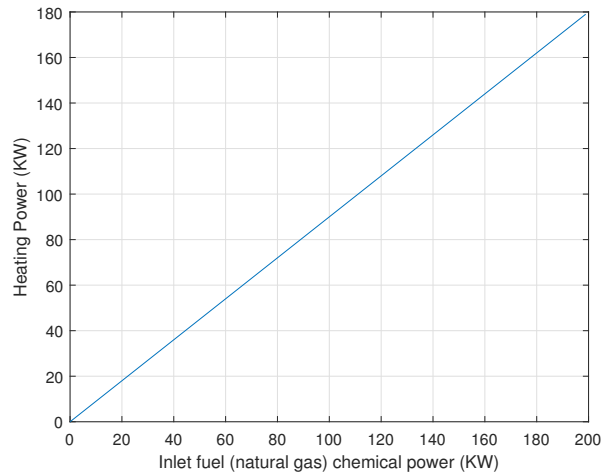


Figure 2.6:  
Heating efficiency curve of the boiler.

### 2.2.4 Absorption Chiller

The absorption chiller (2.7) is able to produce cooling power ( $\Phi_{Abs,C}$ ) by exploiting a heat source ( $\Phi_{Abs,H}$ ) via an absorption refrigeration cycle (usually using a mixture of water and lithium bromide). Its efficiency curve is shown in Figure 2.8.



Figure 2.7:  
An absorption chiller.<sup>4</sup>

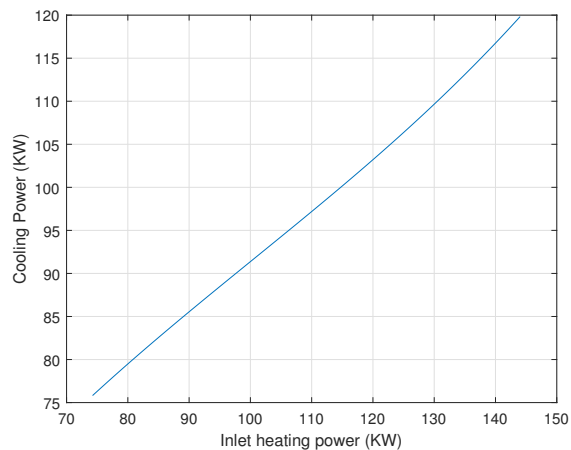


Figure 2.8:  
Cooling efficiency of the absorption chiller.

<sup>3</sup>Viessmann. URL: <https://www.viessmann.it/it/riscaldamento-casa/caldaie-a-condensazione-a-gas/caldaie-a-condensazione-a-gas-murali/caldaia-condensazione-vitodens-200w.html>

<sup>4</sup>Thermotech Green Products. URL: <http://thermotechgp.com/absorption-chiller/>

### 2.2.5 Electric Chiller

The electric chiller (Figure 2.9) employs electricity ( $\Phi_{Chill,E}$ ) to generate cooling power ( $\Phi_{Chill,C}$ ) via a standard refrigeration cycle. Its efficiency curve is displayed in Figure 2.10.

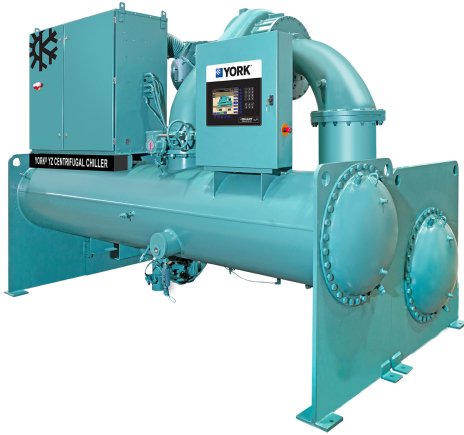


Figure 2.9: An electric chiller.<sup>5</sup>

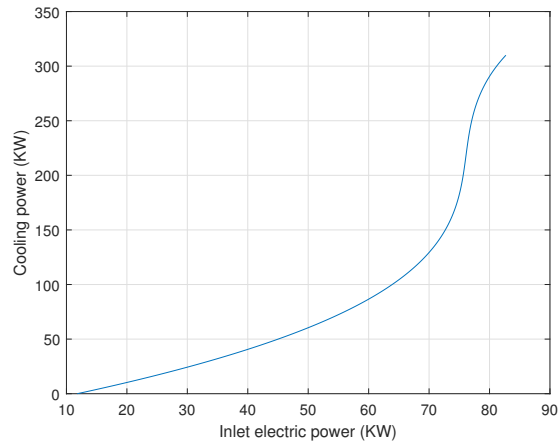


Figure 2.10: Cooling efficiency of the electric chiller.

### 2.2.6 Storage

The system includes storage units (2.11) for heating, cooling and electric power. Thermal storage units are usually tanks equipped with one or two coils for heat exchange, while electric storage units are electrochemical batteries.



(a) A thermal storage tank<sup>6</sup>.



(b) An electricity storage battery<sup>7</sup>.

Figure 2.11: Storage units.

<sup>5</sup>Engineered Systems. URL: <https://www.esmagazine.com/articles/98678-york-yz-magnetic-bearing-centrifugal-chiller-johnson-controls>

<sup>6</sup>Markki Piho. URL: <http://www.markki.com/design/thermal-energy-storage-tanks/>

<sup>7</sup>General Electric. URL: <https://www.ge.com/reports/leading-charge-battery-storage-sweeps-world-ge-finding-place-sun/>

The flux of energy type  $j$  (heat, cooling power or electricity) exiting the storage device at the generic time  $t$  is calculated as:

$$\Phi_{Stor,j}(t) = \frac{E_{Stor,j}(t-1) - E_{Stor,j}(t)}{\Delta T} \quad (2.1)$$

Where  $E_{Stor,j}(t)$  is the quantity of energy stored in the unit at the end of the time-step  $t$ . No energy losses will be considered during the storing process.

### 2.2.7 Photovoltaic

The Photovoltaic panel (2.12) takes advantage of the photoelectric effect of silicon to produce electric power ( $\Phi_{PV}$ ) from solar irradiance. In this work, the forecast on the solar irradiance will be considered exact (not subjected to uncertainty), but in some cases this parameter might also be a source of uncertainty. The electric power produced by the PV is already known, but to have a better idea of its performance it is possible to calculate its efficiency from the data on the solar irradiance, as shown in Figure 2.13:



Figure 2.12:  
A monocrystalline silicon  
PV panel.<sup>8</sup>

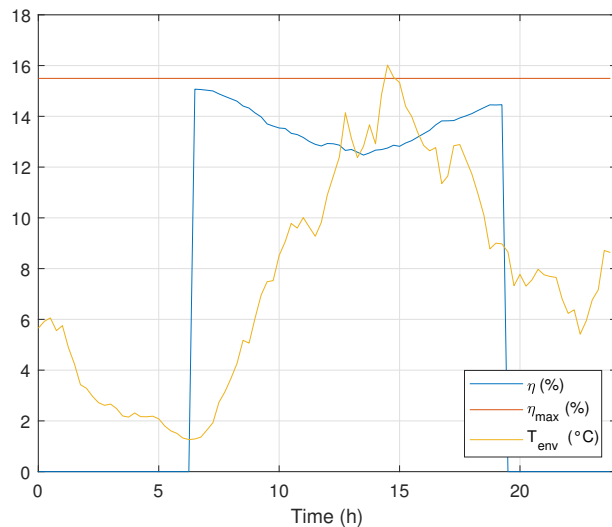


Figure 2.13:  
PV efficiency compared to environment's temperature.

<sup>8</sup>LG. URL: <https://www.lg.com/us/business/solar-panels/lg-lg340n1c-v5#>

## 2.2.8 Wind Turbine

The wind turbine (Figure 2.14) exploits the wind's kinetical energy to produce electric power ( $\Phi_{Wind}$ ).

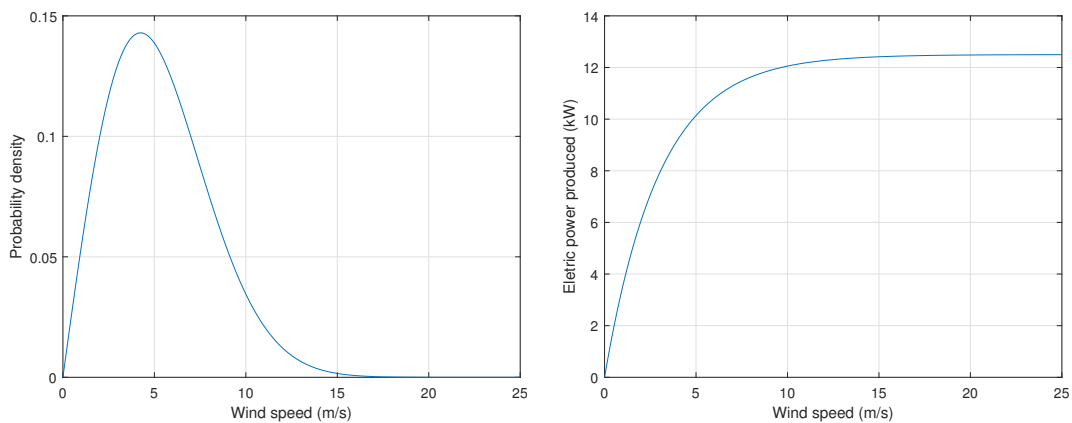


Figure 2.14: A wind turbine.<sup>9</sup>

Only the maximum electric power generated by the turbine ( $\Phi_{Wind,max}$ ) is available. For this reason, the actual power values (as a function of wind speed  $v$ ) will be generated according to a Weibull distribution ( $k = 2, c = 6$ ), displayed in Figure 2.15:

$$f(v) = \frac{k}{c} \left(\frac{v}{c}\right)^{k-1} e^{-\left(\frac{v}{c}\right)^k} \quad (2.2)$$

$$\Phi_{Wind}(v) = \Phi_{Wind,max} \cdot \left(1 - e^{-\frac{v}{c}}\right) \quad (2.3)$$



(a) Weibull distribution of wind speed  $v$ . (b) Electric power as a function of wind speed

Figure 2.15: Wind power values generation method.

<sup>9</sup>Paul Cryan. URL: <https://www.usgs.gov/media/images/wind-turbine-and-forest>

### 2.2.9 Summary

Here is a summary of the consumed and generated power of each component:

<b>Component</b>	<b>Power IN</b>	<b>Power OUT</b>
CHP	Gas	Heat, Electricity
GHP	Gas	Heat, Cool
Boiler	Gas	Heat
Absorption chiller	Heat	Cool
Electric Chiller	Electricity	Cool
PV	Solar irradiance	Electricity
Wind Turbine	Wind's kinetical energy	Electricity
Hot Storage	Heat	Heat
Cold Storage	Cool	Cool
Electricity Storage	Electricity	Electricity

Table 2.1: HRES components summary

# Chapter 3

## The Rolling Horizon method

### 3.1 Background

Model Predictive Control (i.e. Rolling Horizon) was developed independently by Richalet *et al.* (1978) and Cutler and Ramaker (1980), to satisfy the needs of more stringent production requests in the industry.<sup>1</sup> The Rolling Horizon algorithm has been used in process industries (such as oil refineries and chemical plants) since the 1980s, but more recently it has found applications in power electronics and in the balancing of energy systems (such as the one described in this thesis).

### 3.2 Peculiarities of the method

One of the advantages of the Rolling Horizon algorithm is its **adaptability** to many optimization problems characterized by uncertainty: in fact, the algorithm can easily adjust the control system's response if one or more variables in the model are not as predicted.

Furthermore, if implemented correctly, it can greatly **decrease the computational time** of certain types of problem (with respect to other optimization algorithms), since it only forecasts the events contained within a pre-defined *Prediction Horizon* (which can be significantly smaller than the full scope of the problem), and it only actively performs the optimization within the *Control Horizon* (which might be even shorter than the Prediction Horizon). This means that, instead of solving a very large problem, it actually solves several smaller sub-problems (one for each iteration), which might lead to a severe decrease of the computational effort.

However, it follows that the solution that the algorithm computes might not be the optimal one (since a single iteration does not consider the entire time window of the problem): for this reason, the Prediction and Control Horizon have to be chosen wisely to avoid major miscalculations.

---

<sup>1</sup>Giovani Cavalcanti Nunes. *Design and analysis of multivariable predictive control applied to an oil-water-gas separator: a polynomial approach*. 2001. URL: <http://citeseerx.ist.psu.edu/viewdoc/download?doi=10.1.1.6.6300&rep=rep1&type=pdf>,

### 3.3 Algorithm overview

For simplicity's sake, the problem considered in this section as an example will be a plain and straight-forward one: the control of the horizontal trajectory of a vehicle, as it is outlined in Figure 3.1. Let's suppose to be driving a car which needs to follow a given reference trajectory; furthermore, let's imagine to currently be off the correct path, so that the current course of action needs to be corrected by acting on the steering wheel, which is the control system of the vehicle.

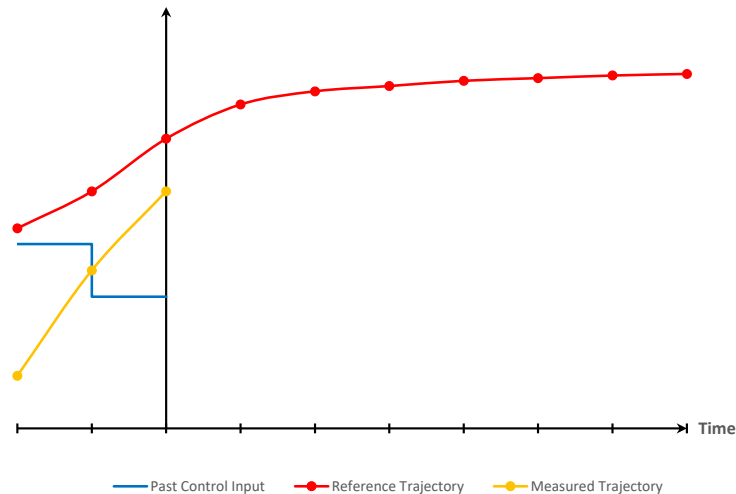


Figure 3.1: Representation of the vehicle problem.

To implement the algorithm, a few parameters have to be defined first.

#### 3.3.1 Time discretization

To be analyzed, the time period under examination needs to be first subdivided into elementary time-steps  $\Delta t$  of constant size: the duration a single time-step must not be too large (otherwise there would be an unacceptable approximation of the phenomenon), and not too small (this would lead to excessive computational times).

#### 3.3.2 Prediction Horizon and Control Horizon

Subsequently, the duration (in time-steps) of the *Prediction Horizon* and the *Control Horizon* needs to be selected. They are defined as follows:

### Prediction Horizon (PH)

The Prediction Horizon (Figure 3.2) is the time period during which the problem relative to a single iteration is analyzed; in other words, the optimization algorithm is going to compute the solution which optimizes the objective function relative to this time-span alone. The duration of the Prediction Horizon must be chosen carefully: if it's too long, the computational effort will be too great (losing this way one of the main advantages of this algorithm); if it's too short, when there is a sudden change in the reference trajectory, the control system might not be able to correct its course in time, or might react too drastically (which is not optimal).

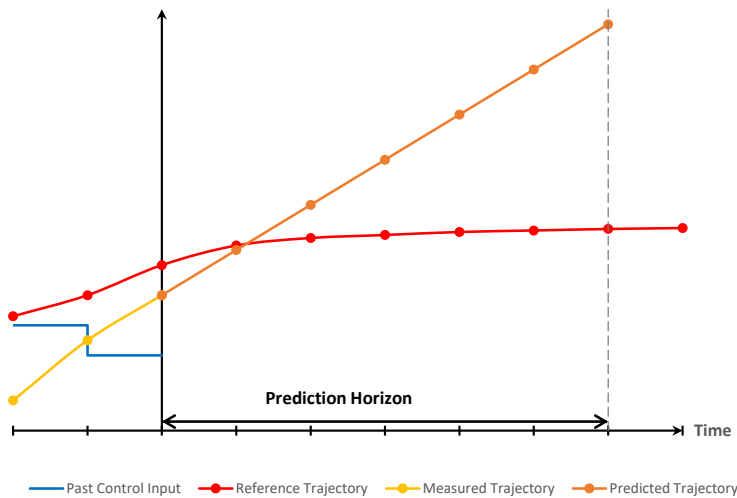


Figure 3.2: Representation of the Prediction Horizon; in this example, it has a size of  $6\Delta t$ . Note that as there is no active control after time 0, the predicted trajectory is a straight line.

### Control Horizon (CH)

The Control Horizon (Figure 3.3) is the time period during which the algorithm can act on the control system; it needs to be equal or shorter than the Prediction Horizon (for obvious reasons: we cannot try to control something we are not able to foresee). It must not be too long (it will lead to a higher complexity of the problem), nor too short (the regulation of the control system might not be optimal, because the algorithm does not have enough degrees of freedom). If the Control Horizon is smaller than the Prediction Horizon, after the CH ends it is assumed that the control input will remain constant throughout the remaining time-steps.

#### 3.3.3 System modelization

An adequate model defining the problem at hand has to be formulated: the nature of this model may vary greatly, depending on the system to be analyzed and the problem itself. Usually it is a set of equations or inequalities describing the physics of the system, plus other mathematical correlations of technical or economical nature.

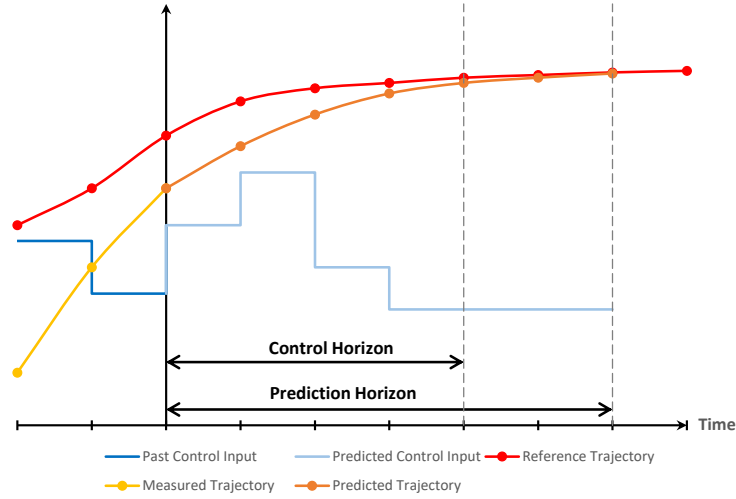


Figure 3.3: An example of implementation of Rolling Horizon. Note that the predicted control input remains constant out of the Control Horizon, which in this case has a size of  $4\Delta t$ .

### 3.3.4 Optimization Problem

Now it is possible to employ the equations of the model described above to define a linear optimization problem, which is often presented in this form:

$$\begin{aligned}
 \min \quad & c' \cdot x \\
 \text{s.a.} \quad & A \cdot x \leq b \\
 & A_{\text{eq}} \cdot x = b_{\text{eq}}
 \end{aligned} \tag{3.1}$$

Where  $x$  is the control variables vector, while  $c'$  is the costs vector; their dot product  $c' \cdot x$  is the objective function. The two systems  $A \cdot x \leq b$  and  $A_{\text{eq}} \cdot x = b_{\text{eq}}$  are the constraints set for the problem. The remainder of this section will be aimed to analyze these elements in greater detail.

#### Control variables

They are the variables which describe the behavior of the control system; the objective of the simulation is to optimize their values in order to minimize the objective function. There may be more than one control variable for each time-step (more degrees of freedom for the control system). In the vehicle example these correspond to the angle at which the steering wheel is turned.

#### Objective function

It is the value which summarizes the effectiveness of the computed solution. It can represent a physical quantity, a monetary value, or any other kind of parameter which needs to be optimized (or even a combination of the three). In the vehicle example, this function may be represented by a fictitious cost times the distance from the reference trajectory, but it can also account, for instance, for the abruptness of the steering (we may not want the curve to be too steep to guarantee the stability of the vehicle or the comfort of the passengers).

### Constraints

They are the conditions which the solution of the problem has to satisfy. They can express physical laws, technical/economical limitations, or other limitations that need to be imposed. They can be hard constraints (they must be satisfied at all costs), or soft constraints (they can be broken, but at a cost which is specified in the objective function). They can be expressed as equations ( $A_{\text{eq}} \cdot x = b_{\text{eq}}$ ) or inequalities ( $A \cdot x \leq b$ ).

### 3.3.5 Application of the algorithm and re-iteration

The solution of the optimization sub-problem within the selected Prediction Horizon will produce a part of the control variables vector  $x$  (ranging from  $t_0 + \Delta t$  to  $t_0 + CH$ , where  $t_0$  is the time of the current iteration). Only the values relative to the first time step (viz.  $x(t_0 + \Delta t)$ ) are actually adopted in the final solution, while the rest are discarded. Afterwards, the current time becomes  $t_0 = t_0 + \Delta t$  and both horizons shift ("roll") of one time-step  $\Delta t$ . The system's current state is measured and, in case it is not the same as the one that was predicted, it is updated. Subsequently, the optimization sub-problem is solved once more and the system's behavior is predicted again by the model using the new data; the process is repeated until the desired time span is reached. A schematic of the process is displayed in Figure 3.4.

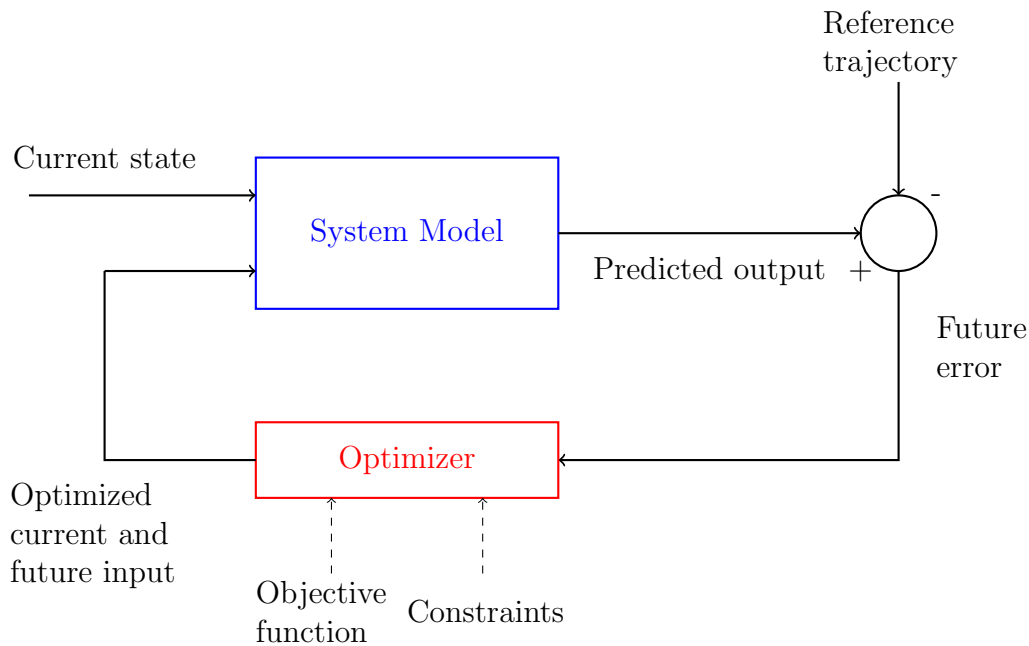


Figure 3.4: Schematization of the Rolling Horizon algorithm.

## 3.4 Application of the algorithm in the case study

### 3.4.1 Time discretization

As stated before, the 24-hour period will be discretized in time-steps of 15 minutes: that means that there is going to be a total of 96 time-steps.

### 3.4.2 Prediction and Control Horizon

In this particular case, there is no need to predict the behavior of the HRES system if it is not possible to regulate it actively: for this reason, the Prediction Horizon and the Control Horizon will be set to the same length.

### 3.4.3 Uncertainty

The problem presents a source of uncertainty: a random variation of  $\pm 10\%$  is implemented at each iteration for the predicted energy demand relative to the current time-step. This will simulate a real-life scenario in which the actual energy consumption varies with respect to the forecast.

### 3.4.4 Flow diagram of the algorithm

The MATLAB algorithm can be summarized as follows:

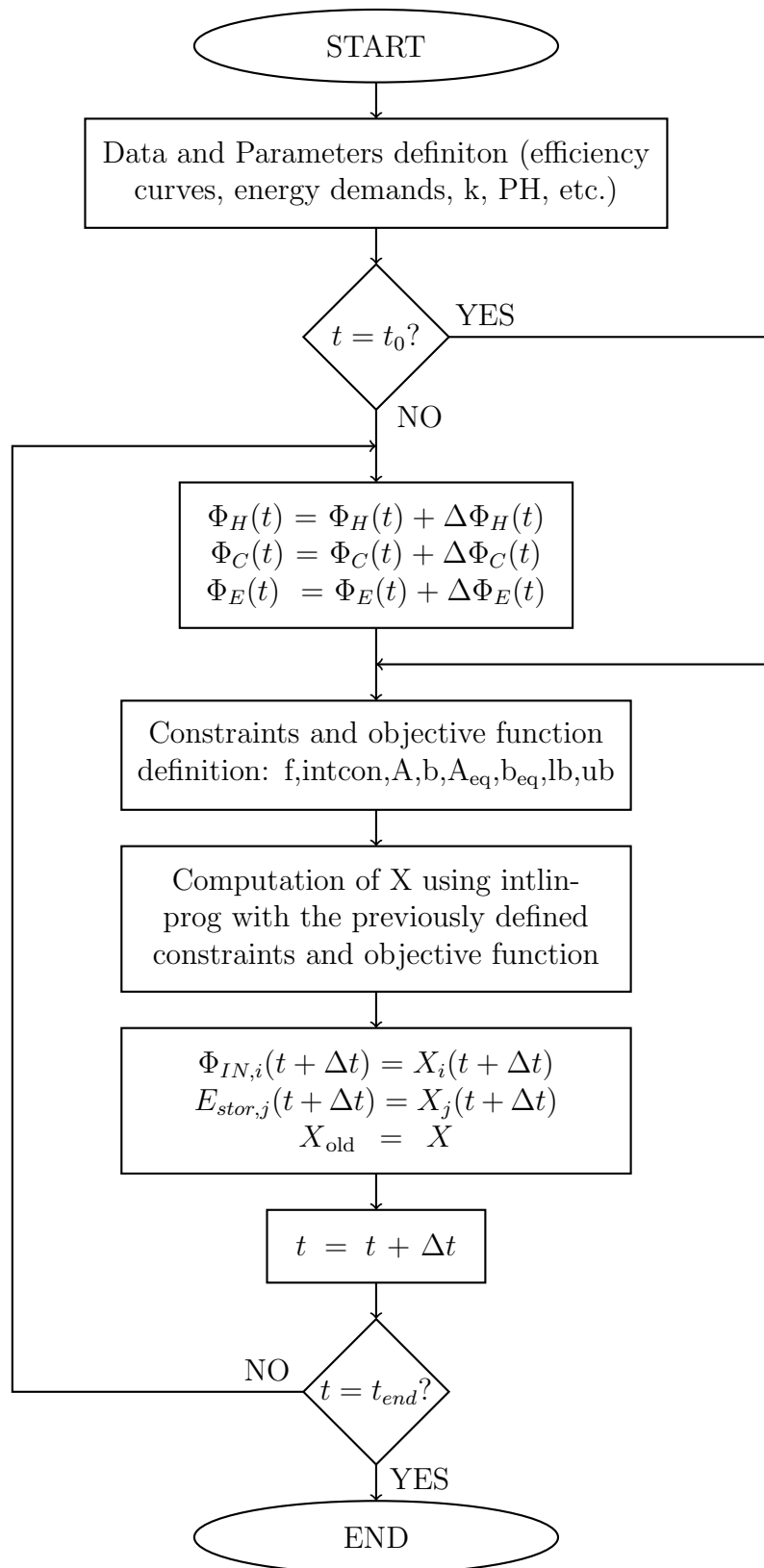


Figure 3.5: Flow diagram of the MATLAB algorithm.



# Chapter 4

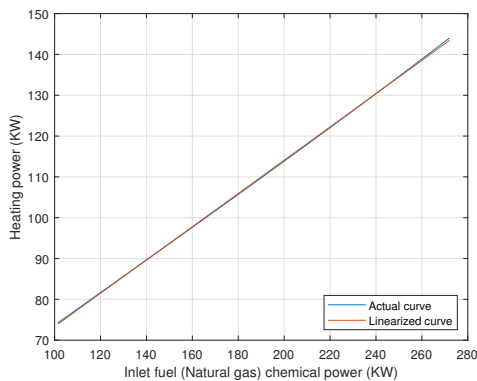
## Optimization problem formulation

### 4.1 Efficiency curves linearization

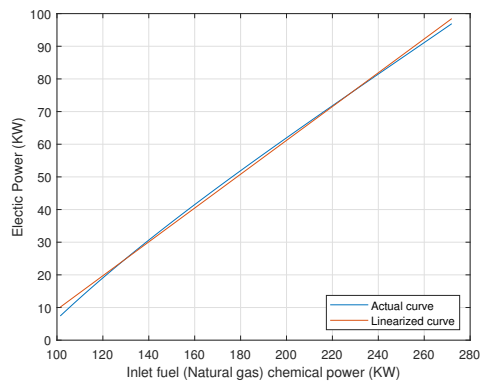
Since the optimization algorithm that is going to be used involves linear programming, the efficiency curves of the components need to be approximated with a first order (linear) polynomial. The power generated by the  $i$ -th component will then be calculated as:

$$\Phi_{OUT,i} = \eta_{0,i} + \eta_{1,i} \cdot \Phi_{IN,i} \quad (4.1)$$

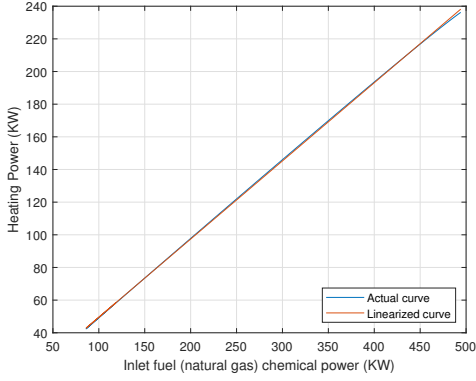
This linearization will not be performed for the boiler (since it's already linear), nor for the PV panels and the wind turbine, which are not going to be part of the control variables, given that they are virtually "cost-free" and they're always consumed when available; moreover, their output power is already known, so there's no need to calculate it. The approximation will be carried out via linear regression of the real efficiency curve. Figure 4.1 shows the linearized curves:



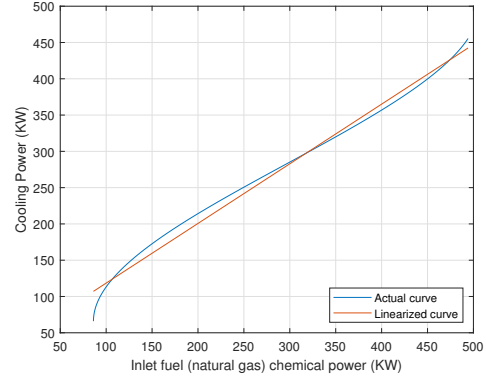
(a) CHP heating efficiency.



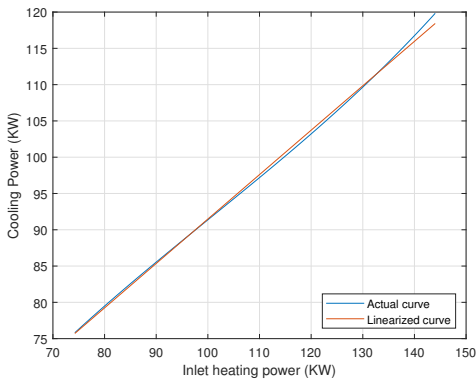
(b) CHP electric efficiency.



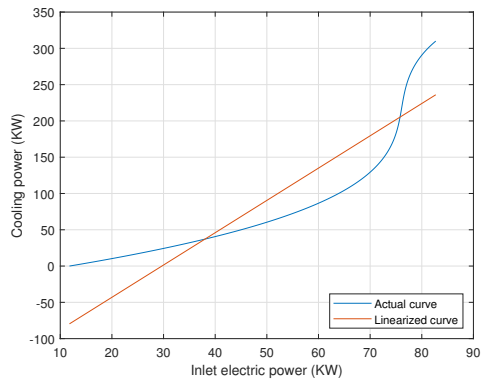
(c) GHP heating efficiency.



(d) GHP cooling efficiency.



(e) Absorption chiller cooling efficiency.



(f) Electric chiller cooling efficiency.

Figure 4.1: Efficiency curves linearization.

## 4.2 Implementation of linear optimization

Now that the model of the system has been defined, the linear optimization problem can be formulated; more specifically, it is possible to write a formulation of the objective function and the linear constraints of the problem. The linear approach has been chosen since it does not require a heavy computational effort (in a real-life scenario, the optimization would need to be performed every 15 minutes).

### 4.2.1 Control variables

The control variables vector  $x$  comprises the values that it is possible to directly modify to influence the system's behavior: the value of  $\Phi_{IN,i}$  of each component (except for  $\Phi_{PV}$  and  $\Phi_{Wind}$ , which are not going to be controlled), the thermal and electric power exchanged with the grids and the storage energy level  $E_{Stor,i}(t)$ .

The vector  $x$  can then be written as:

$$x = \begin{pmatrix} \Phi_{CHP,G} \\ \Phi_{GHP,G} \\ \Phi_{Boil,G} \\ \Phi_{EGrid,in} \\ \Phi_{EGrid,out} \\ \Phi_{TGrid,in} \\ \Phi_{TGrid,out} \\ \Phi_{Abs,H} \\ \Phi_{Chill,E} \\ E_{Stor,H}(t) \\ E_{Stor,C}(t) \\ E_{Stor,E}(t) \end{pmatrix} \quad (4.2)$$

### 4.2.2 Objective function

Now that the control variables are defined, it is possible to assign a cost to each of them. In this case there are no soft constraints, so the objective function will only account for real costs (not fictitious ones): the cost of natural gas, the cost of buying thermal energy and electricity from the grid, and the revenues from selling them. The objective function for each time-step can be written as:

$$\begin{aligned} c' \cdot x &= c_G \cdot (\Phi_{CHP,G} + \Phi_{GHP,G} + \Phi_{Boil,G}) \\ &+ c_E \cdot (\Phi_{EGrid,in} - k \cdot \Phi_{EGrid,out}) \\ &+ c_H \cdot (\Phi_{TGrid,in} - k \cdot \Phi_{TGrid,out}) \end{aligned} \quad (4.3)$$

The coefficient  $k$  is there to account for the difference between the buying and the selling price (usually it's smaller than 1).  $c_G$  and  $c_H$  are calculated from the average price assuming a random variation in a  $\pm 20\%$  range for each time-step.

### 4.2.3 Linear constraints

The problem's constraints can be categorized as:

#### Energy balance constraints

The heating, cooling and electricity balance has to be satisfied at each time-step.

#### *Heating:*

$$\begin{aligned} &\Phi_{CHP,H} + \Phi_{GHP,H} + \Phi_{Boil,H} - \Phi_{Abs,H} + \Phi_{TGrid,in} + \\ & - \Phi_{TGrid,out} - \frac{E_{Stor,H}(t-1) - E_{Stor,H}(t)}{\Delta t} = \Phi_H \end{aligned} \quad (4.4)$$

#### *Cooling:*

$$\Phi_{GHP,C} + \Phi_{Abs,C} + \Phi_{Chill,C} - \frac{E_{Stor,C}(t-1) - E_{Stor,C}(t)}{\Delta t} = \Phi_C \quad (4.5)$$

**Electricity:**

$$\Phi_{CHP,E} - \Phi_{Chill,E} + \Phi_{EGrid,in} - \Phi_{EGrid,out} + \frac{E_{Stor,E}(t-1) - E_{Stor,E}(t)}{\Delta t} = \Phi_E - \Phi_{PV} - \Phi_{Wind} \quad (4.6)$$

Note that  $\Phi_{PV}$  and  $\Phi_{Wind}$  are not variables, but known values.

**Energy conversion via calculated efficiency**

These are the equations correlating the inlet and outlet power of each component  $i$ :

$$\Phi_{OUT,i} = \eta_{0,i} + \eta_{1,i} \cdot \Phi_{IN,i} \quad (4.1)$$

(For the boiler  $\eta_{0,Boil} = 0$ ).

These equations can be integrated in the energy balances, which are rewritten as:

$$\begin{pmatrix} \eta_{1,CHP,H} & \eta_{1,GHP,H} & \eta_{1,Boil} & 0 & 0 & 1 & -1 & -1 & 0 \\ 0 & \eta_{1,GHP,C} & 0 & 0 & 0 & 0 & 0 & \eta_{1,Abs,C} & \eta_{1,Chill,C} \\ \eta_{1,CHP,E} & 0 & 0 & 1 & -1 & 0 & 0 & 0 & -1 \end{pmatrix} \cdot \begin{pmatrix} \Phi_{CHP,G} \\ \Phi_{GHP,G} \\ \Phi_{Boil,G} \\ \Phi_{EGrid,in} \\ \Phi_{EGrid,out} \\ \Phi_{TGrid,in} \\ \Phi_{TGrid,out} \\ \Phi_{Abs,H} \\ \Phi_{Chill,E} \end{pmatrix} + \begin{pmatrix} -\frac{1}{\Delta t} & 0 & 0 & \frac{1}{\Delta t} & 0 & 0 \\ 0 & -\frac{1}{\Delta t} & 0 & 0 & \frac{1}{\Delta t} & 0 \\ 0 & 0 & -\frac{1}{\Delta t} & 0 & 0 & \frac{1}{\Delta t} \end{pmatrix} \cdot \begin{pmatrix} E_{Stor,H}(t) \\ E_{Stor,C}(t) \\ E_{Stor,E}(t) \\ E_{Stor,H}(t-1) \\ E_{Stor,C}(t-1) \\ E_{Stor,E}(t-1) \end{pmatrix} = \begin{pmatrix} \Phi_H - \eta_{0,CHP,H} - \eta_{0,GHP,H} \\ \Phi_C - \eta_{0,GHP,C} - \eta_{0,Abs,C} - \eta_{0,Chill,C} \\ \Phi_E - \Phi_{PV} - \Phi_{Wind} - \eta_{0,CHP,E} \end{pmatrix} \quad (4.7)$$

**Minimum and maximum values**

Each component is characterized by a minimum and a maximum value of power it can produce. Moreover, each storage has a maximum capacity. The constraint on the generic control variable  $x$  can be written as:

$$Min\ value \leq x \leq Max\ value \quad (4.8)$$

In this case the minimum value has to be set equal to 0, and not to the actual minimum power the component is able to generate, because that would mean it is always functioning.

### 4.3 Issues with linear optimization

The implementation of linear optimization poses several issues, which might lead to a non-accurate or non-optimal solution.

#### 4.3.1 Efficiency's zero-degree term

As stated before, a component's generated power is calculated as:

$$\Phi_{OUT,i} = \eta_{0,i} + \eta_{1,i} \cdot \Phi_{IN,i} \quad (4.1)$$

The issue with this formulation is that it provides an inaccurate estimate of the output power when  $\Phi_{IN,i}$  assumes values that are equal or close to 0. This is due to the fact that the linear fit is calculated in the interval  $[\Phi_{min,i}, \Phi_{max,i}]$ , so it does not accurately approximate the curve outside of that range.

As an example, let us consider the CHP: its electric efficiency coefficients are  $\eta_{0,CHP,E} \approx -8.5$  and  $\eta_{1,CHP,E} \approx 0.5$ . Let us suppose to have a value of  $\Phi_{CHP,G} = 1kW$ : that means that the produced electric power would be  $\Phi_{CHP,E} = -8.5 + 0.5 \cdot 1 = -8kW$ , which is not only unrealistic, but physically impossible.

#### 4.3.2 Minimum value of variables

To avoid the previous issue, one might impose a minimum value for  $\Phi_{IN,i}$  which is sufficiently high (for example  $\Phi_{min,i}$ , since we know that each component has a minimum amount of power it can generate), but that would force this component to be always on: simple linear programming is not able to discriminate between OFF and ON states of components.

#### 4.3.3 Inaccurate linear efficiency

For some components like the electric chiller or the GHP, a linear fit of the efficiency curve doesn't approximate the component's behavior in an accurate way; employing a piecewise linear approximation or using a higher order polynomial is not possible since the constraints and the objective function's equations have to be strictly linear.

## 4.4 Implementation of MILP optimization

To solve the previously described issues, it is possible to exploit the Mixed Integer Linear Programming (MILP) approach: it involves the implementation of integer variables, in addition to the linear ones described previously. In particular, for this study's purposes the integer variables are going to be binary.

#### 4.4.1 Definition of the binary variables

A binary variable  $Y_i$  is assigned to each component  $i$  of the HRES system (except for the boiler, the storage and the grids): it will have to be equal to 1 when the component is on, equal to 0 when it is off.

The control variables vector  $x$  then becomes:

$$x = \begin{pmatrix} \Phi_{CHP,G} \\ \Phi_{GHP1,G} \\ \Phi_{GHP2,G} \\ \Phi_{Boil,G} \\ \Phi_{EGrid,in} \\ \Phi_{EGrid,out} \\ \Phi_{TGrid,in} \\ \Phi_{TGrid,out} \\ \Phi_{Abs,H} \\ \Phi_{Chill,E} \\ E_{Stor,H}(t) \\ E_{Stor,C}(t) \\ E_{Stor,E}(t) \\ Y_{CHP} \\ Y_{GHP1} \\ Y_{GHP2} \\ Y_{Abs} \\ Y_{Chill1} \\ Y_{Chill2} \\ Y_{Chill3} \end{pmatrix} \quad (4.9)$$

#### 4.4.2 Additional constraints

To make the binary variable follow the behavior of the  $i$ -th component, two additional constraints have to be set:

$$\Phi_i \geq \Phi_{min,i} \cdot Y_i \quad (4.10)$$

$$\Phi_i \leq \Phi_{max,i} \cdot Y_i \quad (4.11)$$

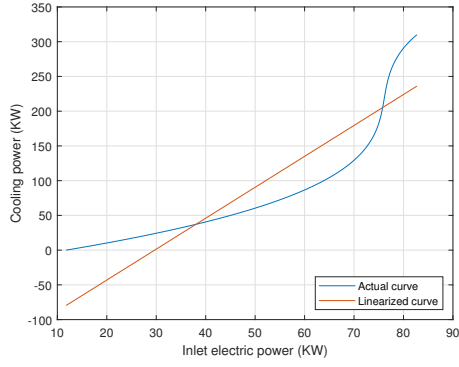
This way, when  $Y_i = 0$  (OFF state) the component's power will be forced to 0, when  $Y_i = 1$  (ON state) the component's power will be limited in the interval  $[\Phi_{min}, \Phi_{max}]$ . This means that the previously set constraints for these values (i.e. equation 4.8) have become redundant, so they can be discarded.

Furthermore, it is possible to employ the binary variables to make sure that when a component's inlet power is 0, the generated power value is not influenced by the zero-degree term of the efficiency  $\eta_{0,i}$ ; this way, equation 4.1 becomes:

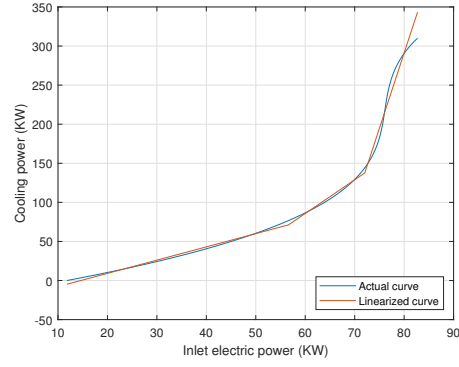
$$\Phi_{OUT,i} = \eta_{0,i} \cdot Y_i + \eta_{1,i} \cdot \Phi_{IN,i} \quad (4.12)$$

#### 4.4.3 Piecewise linearization of efficiency curves

Now it is also possible to implement a piecewise linear regression of the efficiency curve of the electric chiller and of the cooling efficiency curve of the gas heat pump (Figures 4.2 and 4.3):

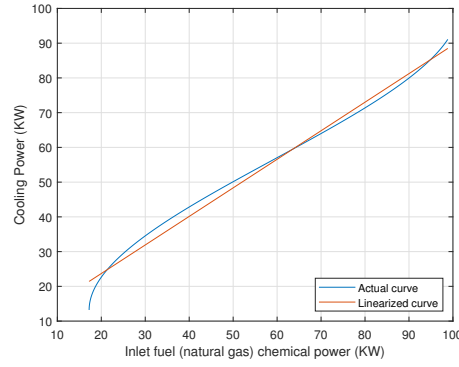


(a) One-piece linear regression

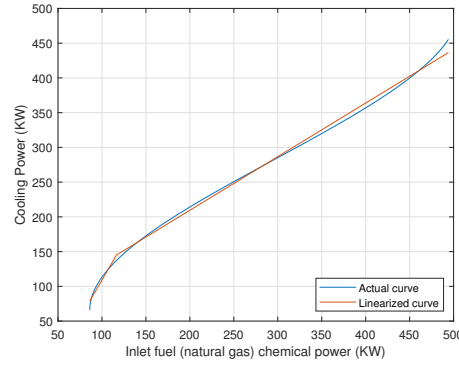


(b) Three-piece linear regression

Figure 4.2: Comparison between one-piece and three-piece linear fit of the chiller's efficiency



(a) One-piece linear regression



(b) Two-piece linear regression

Figure 4.3: Comparison between one-piece and two-piece linear fit of the gas heat pump's cooling efficiency

The distinct pieces of the curve will be treated as separate components by the algorithm, but it is necessary to impose an additional constraint to make sure that only one of them is active at any given time:

$$Y_{chill1} + Y_{chill2} + Y_{chill3} \leq 1 \quad (4.13)$$

$$Y_{GHP1} + Y_{GHP2} \leq 1 \quad (4.14)$$

#### 4.4.4 Inequality constraints

The inequality constraints of the system for every time-step can now be written as:

$$\begin{pmatrix}
 -1 & 0 & 0 & 0 & 0 & 0 & 0 \\
 1 & 0 & 0 & 0 & 0 & 0 & 0 \\
 0 & -1 & 0 & 0 & 0 & 0 & 0 \\
 0 & 1 & 0 & 0 & 0 & 0 & 0 \\
 0 & 0 & -1 & 0 & 0 & 0 & 0 \\
 0 & 0 & 1 & 0 & 0 & 0 & 0 \\
 0 & 0 & 0 & -1 & 0 & 0 & 0 \\
 0 & 0 & 0 & 1 & 0 & 0 & 0 \\
 0 & 0 & 0 & 0 & -1 & 0 & 0 \\
 0 & 0 & 0 & 0 & 1 & 0 & 0 \\
 0 & 0 & 0 & 0 & 0 & -1 & 0 \\
 0 & 0 & 0 & 0 & 0 & 1 & 0 \\
 0 & 0 & 0 & 0 & 0 & 0 & -1 \\
 0 & 0 & 0 & 0 & 0 & 0 & 1 \\
 0 & 0 & 0 & 0 & 0 & 0 & 0 \\
 0 & 0 & 0 & 0 & 0 & 0 & 0
 \end{pmatrix} \cdot \begin{pmatrix}
 \Phi_{CHP,G} \\
 \Phi_{GHP1,G} \\
 \Phi_{GHP2,G} \\
 \Phi_{Abs,H} \\
 \Phi_{Chill1,E} \\
 \Phi_{Chill2,E} \\
 \Phi_{Chill3,E}
 \end{pmatrix} +$$

$$+ \begin{pmatrix}
 \Phi_{CHP,G,min} & 0 & 0 & 0 \\
 -\Phi_{CHP,G,max} & 0 & 0 & 0 \\
 0 & \Phi_{GHP1,G,min} & 0 & 0 \\
 0 & -\Phi_{GHP1,G,max} & 0 & 0 \\
 0 & 0 & \Phi_{GHP1,G,min} & 0 \\
 0 & 0 & -\Phi_{GHP1,G,max} & 0 \\
 0 & 0 & 0 & \Phi_{Abs,H,min} \\
 0 & 0 & 0 & -\Phi_{Abs,H,max} \\
 0 & 0 & 0 & 0 \\
 0 & 0 & 0 & 0 \\
 0 & 0 & 0 & 0 \\
 0 & 0 & 0 & 0 \\
 0 & 0 & 0 & 0 \\
 0 & 0 & 0 & 0 \\
 0 & 0 & 0 & 0 \\
 0 & 0 & 0 & 0 \\
 0 & 1 & 1 & 0 \\
 0 & 0 & 0 & 0
 \end{pmatrix} \cdot \begin{pmatrix}
 Y_{CHP} \\
 Y_{GHP1} \\
 Y_{GHP2} \\
 Y_{Abs}
 \end{pmatrix} +$$

$$+ \begin{pmatrix} 0 & 0 & 0 \\ 0 & 0 & 0 \\ 0 & 0 & 0 \\ 0 & 0 & 0 \\ 0 & 0 & 0 \\ \Phi_{Chill1,E,min} & 0 & 0 \\ -\Phi_{Chill1,E,max} & 0 & 0 \\ 0 & \Phi_{Chill2,E,min} & 0 \\ 0 & -\Phi_{Chill2,E,max} & 0 \\ 0 & 0 & -\Phi_{Chill3,E,min} \\ 0 & 0 & \Phi_{Chill3,E,max} \\ 0 & 0 & 0 \\ 1 & 1 & 1 \end{pmatrix} \cdot \begin{pmatrix} Y_{Chill1} \\ Y_{Chill2} \\ Y_{Chill3} \end{pmatrix} \leq \begin{pmatrix} 0 \\ 0 \\ 0 \\ 0 \\ 0 \\ 0 \\ 0 \\ 0 \\ 0 \\ 0 \\ 0 \\ 1 \\ 1 \end{pmatrix} \tag{4.15}$$

To have a better understanding of the size of the problem, it might be useful to estimate how many inequalities make up the constraints: there are 2 inequalities for each component (minimum and maximum power constraints) and 1 inequality for each component whose curve has been piecewise linearized; this means that, for each time-step of the Prediction Horizon, there are 16 inequality constraints with 11 variables.

### 4.4.5 Equality constraints

The equality constraints of the problem consist of the three energy balance equations for every time-step and are formulated as:

$$\begin{aligned}
 & \begin{pmatrix} \eta_{1,CHP,H} & \eta_{1,GHP,H} & \eta_{1,GHP,H} & \eta_{1,Boil} & 0 & 0 & 1 & -1 & -1 \\ 0 & \eta_{1,GHP1,C} & \eta_{1,GHP2,C} & 0 & 0 & 0 & 0 & 0 & \eta_{1,Abs,C} \\ \eta_{1,CHP,E} & 0 & 0 & 0 & 1 & -1 & 0 & 0 & 0 \end{pmatrix} \cdot \begin{pmatrix} \Phi_{CHP,G} \\ \Phi_{GHP1,G} \\ \Phi_{GHP2,G} \\ \Phi_{Boil,G} \\ \Phi_{EGrid,in} \\ \Phi_{EGrid,out} \\ \Phi_{TGrid,in} \\ \Phi_{TGrid,out} \\ \Phi_{Abs,H} \end{pmatrix} + \\
 & + \begin{pmatrix} 0 & 0 & 0 \\ \eta_{1,Chill1,C} & \eta_{1,Chill2,C} & \eta_{1,Chill3,C} \\ -1 & -1 & -1 \end{pmatrix} \cdot \begin{pmatrix} \Phi_{Chill1,E} \\ \Phi_{Chill2,E} \\ \Phi_{Chill3,E} \end{pmatrix} + \\
 & + \begin{pmatrix} -\frac{1}{\Delta t} & 0 & 0 & \frac{1}{\Delta t} & 0 & 0 \\ 0 & -\frac{1}{\Delta t} & 0 & 0 & \frac{1}{\Delta t} & 0 \\ 0 & 0 & -\frac{1}{\Delta t} & 0 & 0 & \frac{1}{\Delta t} \end{pmatrix} \cdot \begin{pmatrix} E_{Stor,H}(t) \\ E_{Stor,C}(t) \\ E_{Stor,E}(t) \\ E_{Stor,H}(t-1) \\ E_{Stor,C}(t-1) \\ E_{Stor,E}(t-1) \end{pmatrix} + \\
 & + \begin{pmatrix} \eta_{0,CHP,H} & \eta_{0,GHP,H} & \eta_{0,GHP,H} & 0 \\ 0 & \eta_{0,GHP1,C} & \eta_{0,GHP2,C} & \eta_{0,Abs,C} \\ \eta_{0,CHP,E} & 0 & 0 & 0 \end{pmatrix} \cdot \begin{pmatrix} Y_{CHP} \\ Y_{GHP1} \\ Y_{GHP2} \\ Y_{Abs} \end{pmatrix} + \\
 & + \begin{pmatrix} 0 & 0 & 0 \\ \eta_{0,Chill1,C} & \eta_{0,Chill2,C} & \eta_{0,Chill3,C} \\ 0 & 0 & 0 \end{pmatrix} \cdot \begin{pmatrix} Y_{Chill1} \\ Y_{Chill2} \\ Y_{Chill3} \end{pmatrix} = \\
 & = \begin{pmatrix} \Phi_H \\ \Phi_C \\ \Phi_E - \Phi_{PV} - \Phi_{Wind} \end{pmatrix}
 \end{aligned} \tag{4.16}$$

Note that, for the first time-step, the variable  $E_{Stor,i}(t)$  does not exist: it is instead replaced by the known value  $E_{Stor,i}(0)$  (i.e. the initial amount of energy stored), which is set equal to 0 for all three storage units.

In this case, for each time-step of the Prediction Horizon, there are 3 equality constraints with 25 variables.

### 4.4.6 Implementation in MATLAB

The MILP optimization will be performed by using MATLAB's built-in function `intlinprog`. The function's syntax is presented in this form:

```
x = intlinprog(f,intcon,A,b,Aeq,beq,lb,ub,x0,options)
```

Where:

- `intcon` is the vector specifying which variables are integer;
- $A \cdot x \leq b$  is the system of inequality constraints (i.e. equations 4.10, 4.11, 4.12);
- $Aeq \cdot x = beq$  is the system of equality constraints (i.e. equation 4.16);
- `lb` and `ub` are the vectors specifying the minimum and maximum value of each variable;
- `x0` is the starting point of the optimization which must be a feasible solution: in this study, it is not possible to use the previous iteration's solution as a starting point because the energy demand changes every time, rendering the past solution unfeasible;
- `options` is an object specifying the options for `intlinprog`, such as the optimization's tolerance or the heuristics of the algorithm.



# Chapter 5

## Optimization results

The optimization's results are going to vary based on the following parameters:

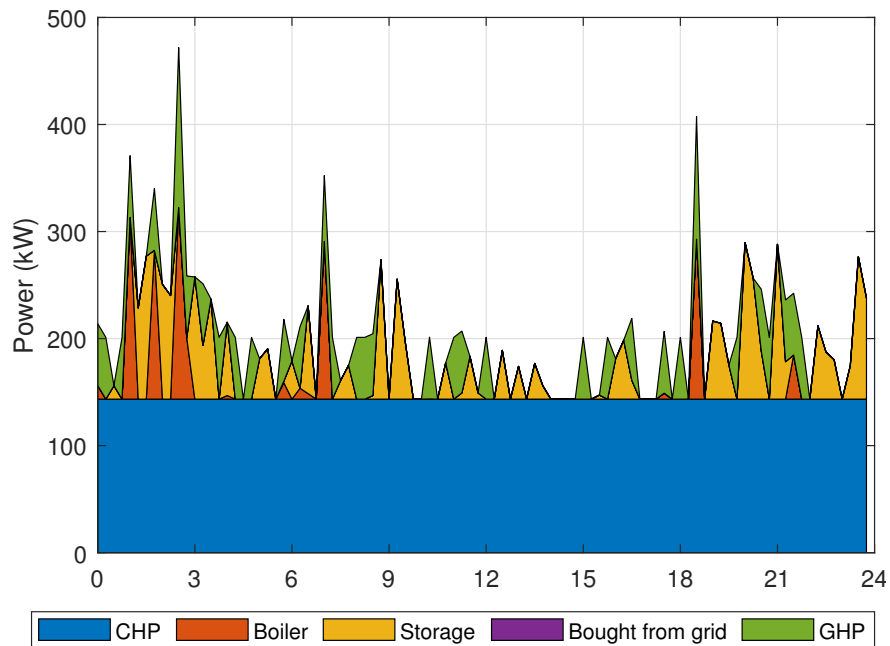
- The uncertainty associated to the energy demand and the method used to generate it;
- The coefficient  $k$ , which affects both the electricity and the thermal energy's selling price (the higher  $k$ , the higher the revenues);
- The size of the Prediction Horizon  $PH$  (which is also equal to the size of the Control Horizon  $CH$ ) that will heavily affect computational times and the objective function's value.

For the preliminary optimization, the following values are going to be adopted:  $k = 0.3$ ,  $PH = CH = 60$ . Later on, a sensitivity analysis on these parameters will follow.

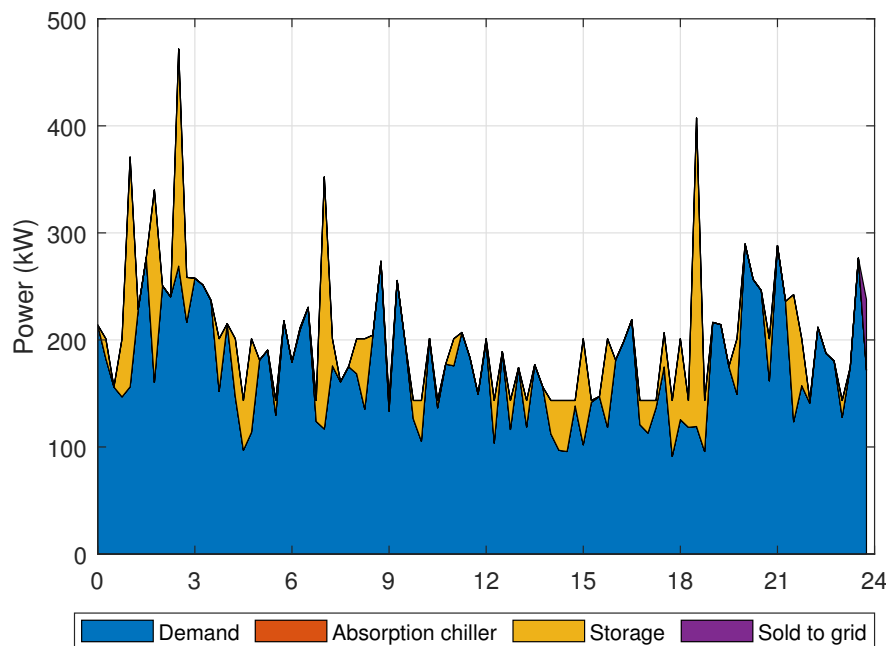
## 5.1 Results of the optimization

### 5.1.1 Heating

As shown in Figure 5.1, the CHP significantly contributes to cover the energy demand (in fact it is always producing the maximum power), while the other components are used to make up for the remaining power peaks. No thermal energy is bought from the grid, and very little is sold to it.



(a) Heating production.

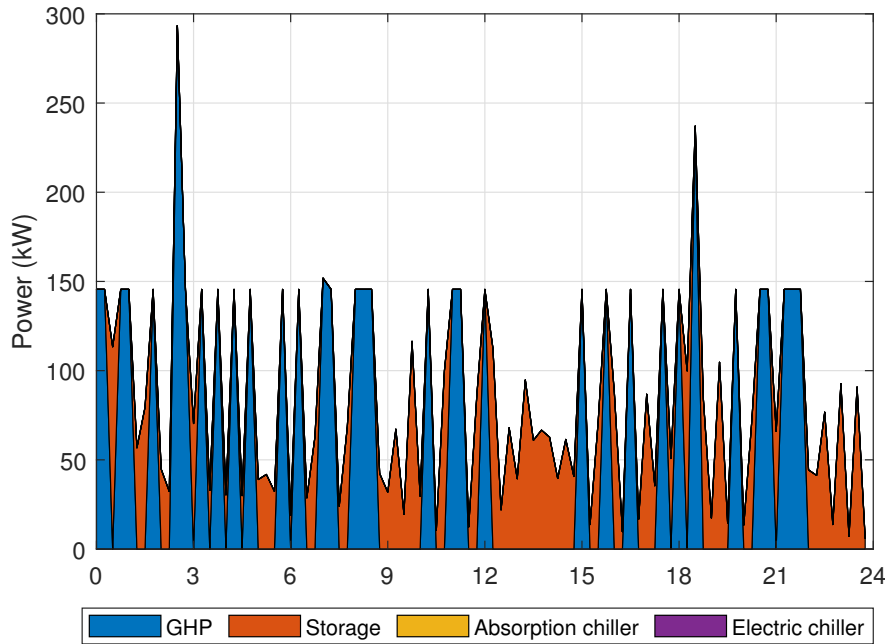


(b) Heating demand.

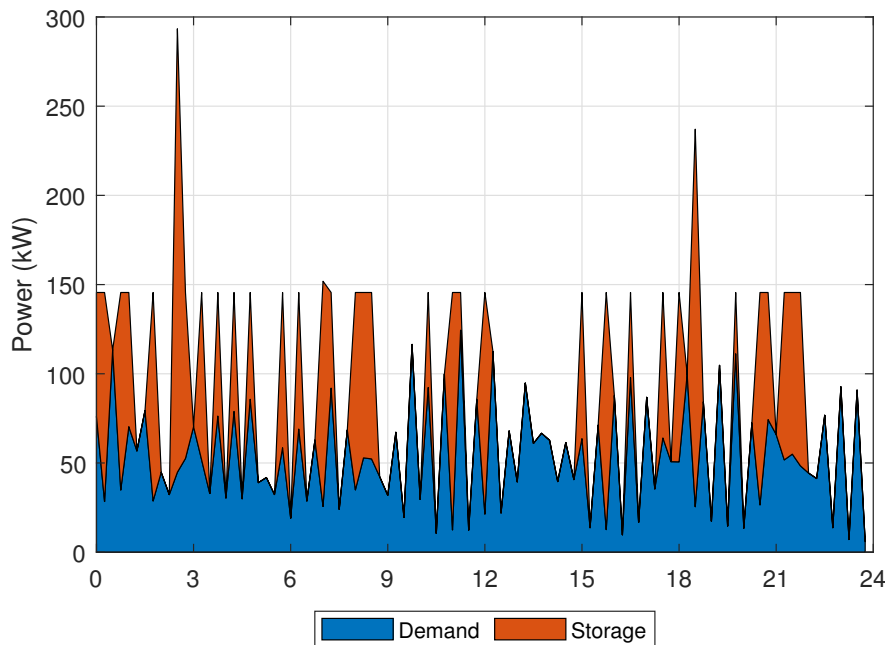
Figure 5.1: Results for heating power.

### 5.1.2 Cooling

As shown in Figure 5.2, the GHP and the storage are used to cover the demand, while the electric and the absorption chiller are never used.



(a) Cooling production.



(b) Cooling demand.

Figure 5.2: Results for cooling power.

### 5.1.3 Electricity

As shown in Figure 5.3, the CHP and the PV are the components that contribute the most to the power generation, while wind power generates a modest amount. The storage is mainly used with the purpose of selling electricity when the price is highest. The wind turbine has a marginal role in contributing to the total electric power generation. No electricity is bought from the grid.

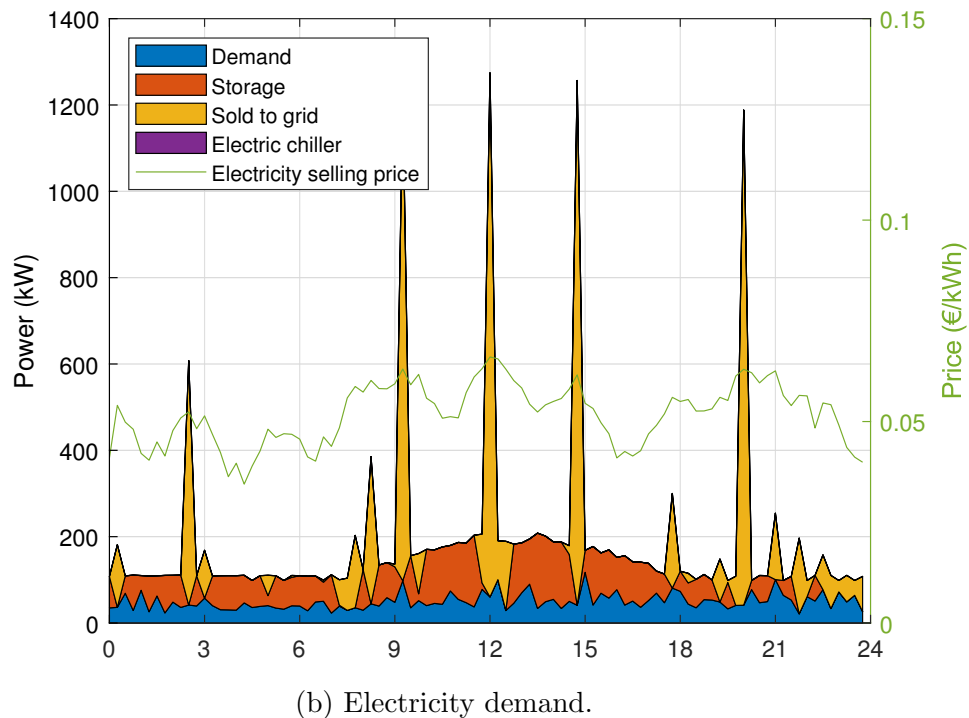
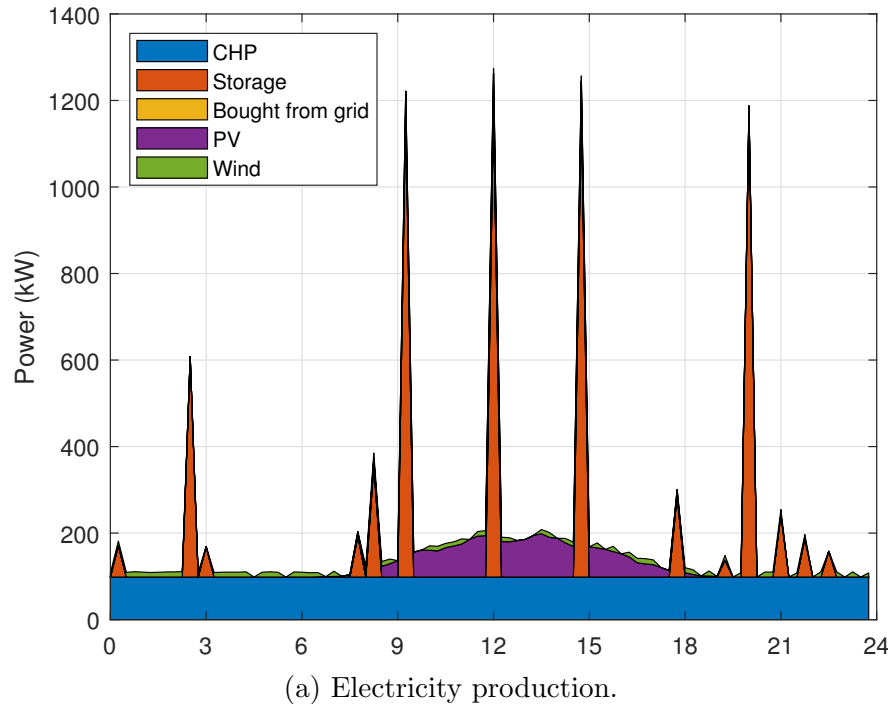


Figure 5.3: Results for electric power.

### 5.1.4 Storage

Figure 5.4 shows the usage of the storage units during the day. Heat storage is mainly used in the evening, while cooling storage is used in the morning. The electric storage unit presents several fluctuations during the day, corresponding to the moments in which power is sold to the grid.

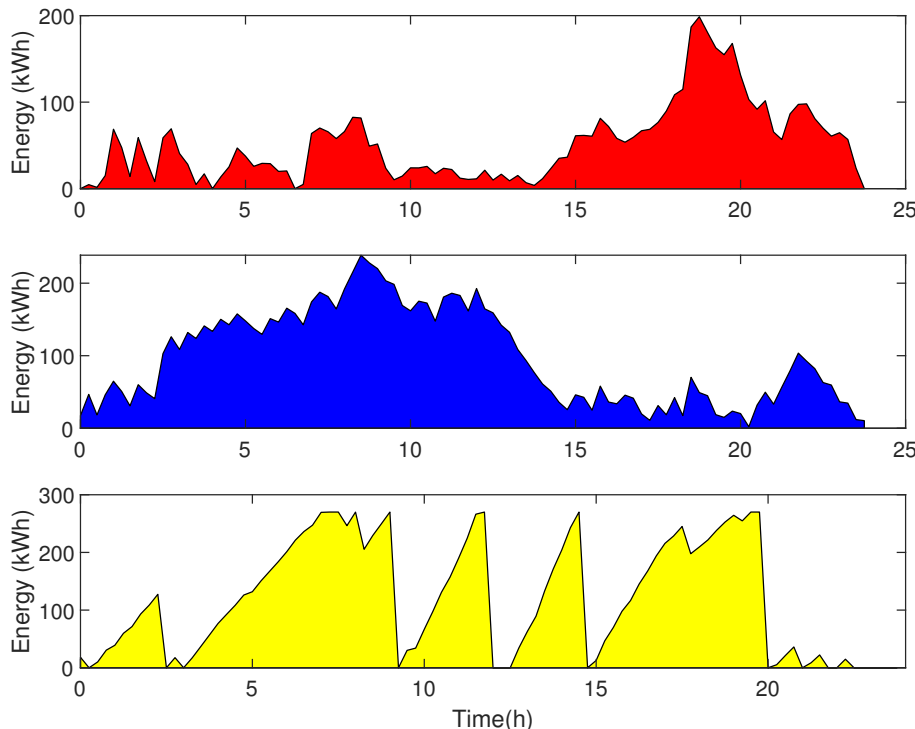


Figure 5.4: Energy cumulated in the heating (red), cooling (blue) and electric (yellow) storages.

## 5.2 Considerations

The most frequently used component of the system is the CHP: this is not surprising, since it is able to produce heat and electricity, both of which have the option of being sold to the grid, while the coefficient  $k$  is high enough to make this economically profitable. Since the heating power required by the user is often higher than the electric power demand, electricity production is significantly higher than the user's request, allowing for an effective use of the storage system to sell electricity when it's most convenient.

The only component which is used to cover the cooling demand is the GHP: this is probably because it is more convenient to sell electricity than to use it to power the electric chiller; at the same time, since heating demand is already very high, rather than raising it even further by using the absorption chiller, the algorithm chooses to increase the consumption of natural gas to fuel the GHP.

It is also possible to calculate the penetration of renewables for electricity production in this specific scenario, as:

$$\text{Renewables penetration} = \frac{\text{Electricity produced by PV and wind turbine}}{\text{Total electricity produced}} \quad (5.1)$$

The value calculated using this formula is 24,78%. It could be higher if the system included a component capable of generating heating power using renewable energy (such as a thermal solar panel or a fuel cell/electrolyzer): this way, it wouldn't need to resort to the CHP as its main source of heat production (which subsequently influences electricity production).

### 5.3 Assessment of the algorithm's effectiveness

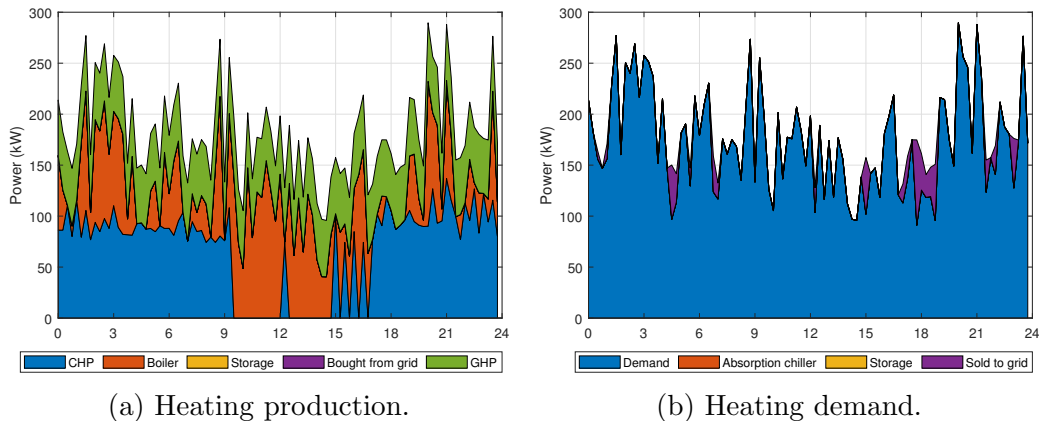
The daily cost calculated using this algorithm is €35.33; to evaluate the efficacy of the optimization, one might want to compare it with a scenario where the system's operation is not aided by the Rolling Horizon algorithm: the difference between the objective function's values in the two cases will be a significant benchmark.

#### Comparison with priority order method

A good way to perform the HRES system's operation without an optimization algorithm might be to establish a priority order of the system's components: the most efficient ones are the first ones to be employed, while the others cover the (eventual) remaining demand. The priority of the components has been decided according to the results obtained during the Rolling Horizon optimization:

- **Electricity:** the PV panel and the wind turbine's generated power is the first one to be used to cover the demand; if it is higher than the demand, the remaining part is sold to the grid, if it is lower, the remaining demand is covered by the combined heat and power unit; in case the three components are not enough to cover the demand, additional power is bought from the grid.
- **Cooling:** the gas heat pump has the highest priority, followed by the electric chiller and by the absorption chiller.
- **Heating:** heat generated by the CHP and the GHP is used first in this case, while the boiler covers the remaining demand; in case the three components are not enough to cover the demand, additional power is bought from the grid.

The results obtained using this method are displayed in Figure 5.5:



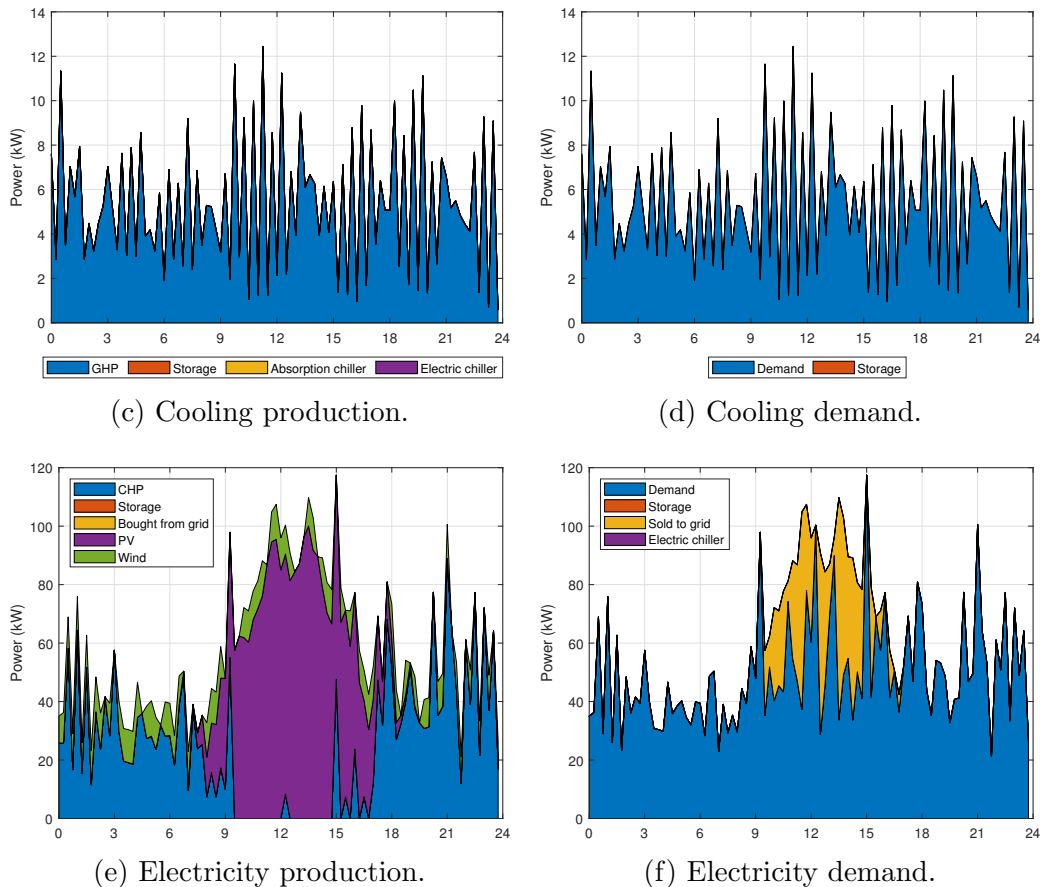


Figure 5.5: Results of the priority order simulation.

The most evident aspect of this method is that the storage units are never used, since there is no prediction of the future demands; moreover, no energy is bought from the grid, while in certain cases it is sold, but the amount is not comparable to the Rolling Horizon simulation. The value of the objective function calculated using this method is €124.72, resulting in a 253% increase when compared to the Rolling Horizon optimization cost.

### 5.3.1 Comparison with standard MILP optimization

An alternative way of optimizing the control of the HRES without resorting to the Rolling Horizon method might be the solution of a single MILP problem on the whole time period under examination, using the predicted energy demand values and not accounting for uncertainty. The following results (Figure 5.6) were obtained using this method:

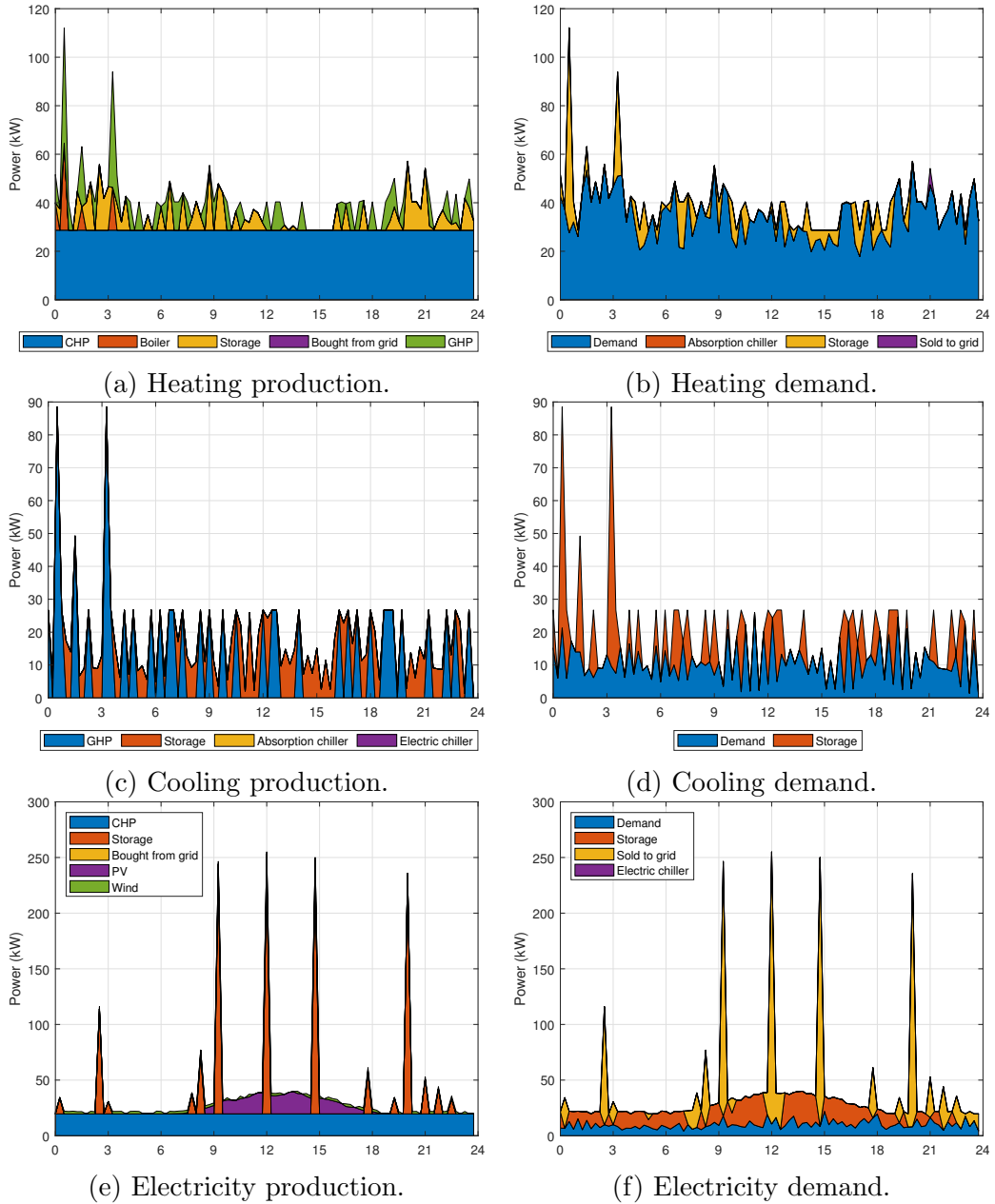


Figure 5.6: Results of the standard MILP optimization.

The resulting scenario is not too different from the one simulated using the Rolling Horizon algorithm and the calculated objective function is even lower: €35.27; however, this type of simulation does not account for the forecast’s uncertainty, so the entire optimization is performed using the data available at the first time-step. This results in differences between the predicted energy requirements and the actual ones, which are managed as follows:

- If heat generation is higher than the actual demand for that specific time-step, the difference is sold to the district heating grid; otherwise, the boiler will cover for the remaining demand (cheaper than buying from the grid);
- If cooling generation is higher than the actual demand for that specific time-step, the difference is lost; otherwise the electric chiller will cover for the remaining demand (since the minimum cooling power of the electric chiller is

0, it allows for greater flexibility with small energy demands). The electric power required will be bought from the grid;

- If the electricity generation is higher than the actual demand for that specific time-step, the difference is sold to the national grid; otherwise, it will be bought from it.

By considering these additional costs, it is possible to calculate a difference of €42.05 from the predicted value, resulting in a total cost of €77.33; this amounts to a 119% increase when compared to the Rolling Horizon simulation's objective function; note that most of the additional cost is due to the extra cooling demand, since it is the most costly type of energy to produce and it is not possible to buy it from the grid.

## 5.4 Error due to linearization

The linearization of the components' efficiency curves will generate an error due to the approximation; it is possible to estimate this error by:

- Interpolating the values of  $\Phi_{OUT,i}$  calculated with the linearized efficiency, with the values of the original efficiency curves (obtaining the "corrected"  $\Phi_{IN,i}$ );
- Evaluating the "corrected" objective function using the interpolated values;
- Calculating the error of the computed objective function relative to the "corrected" one.

Following this procedure, the error is calculated as:

$$\frac{|Computed\ objective\ function - Corrected\ objective\ function|}{|Corrected\ objective\ function|} \quad (5.2)$$

The relative error, for  $PH = 60$  and  $k = 0.3$ , is 14%, while the absolute error is €5.79. This value is very small when compared to the difference between the Rolling Horizon optimization result and the one obtained using different algorithm, so it can be deemed acceptable.



# Chapter 6

## Sensitivity analyses results

To perform the sensitivity analysis on the algorithm's most relevant parameters, the uncertainty will not be generated randomly every time, but it will be the same for every simulation. This way, there will be no external factors to influence the results.

### 6.1 Sensitivity analysis on the Prediction Horizon

The sensitivity analysis on the Prediction Horizon is going to take into account two main parameters: the obtained value of the objective function and the computational time. The parameter  $k$  (corresponding to the energy selling/buying price ratio) will be set equal to 0.3 for all iterations.

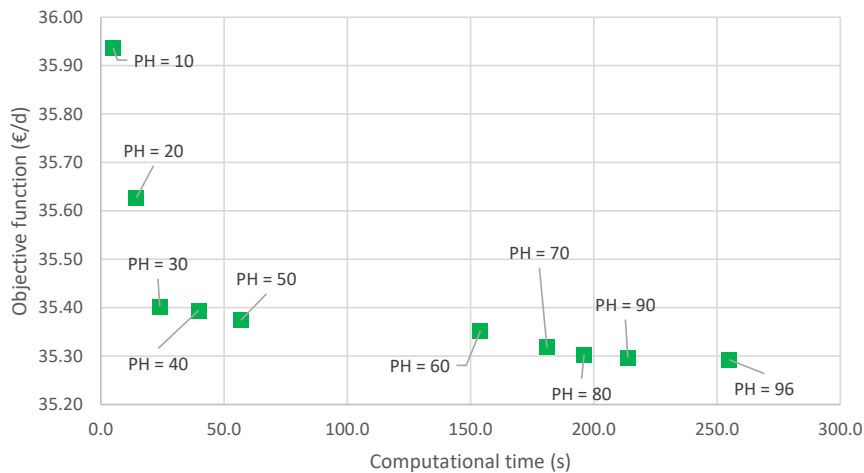


Figure 6.1: Sensitivity analysis on the parameter  $PH$ .

The overall trend (Figure 6.1) is easy to observe: the objective function becomes lower with the increase of  $PH$  (because it optimizes a larger time-window at each iteration, thus obtaining a "better" solution), while the computational time gets higher (because it involves solving more complex problems).

## 6.2 Sensitivity analysis on selling/buying price ratio

The sensitivity analysis on the coefficient  $k$  will be performed by keeping  $PH$  constant and equal to 60. The value of the objective function will be representative of the effect of varying this parameter.

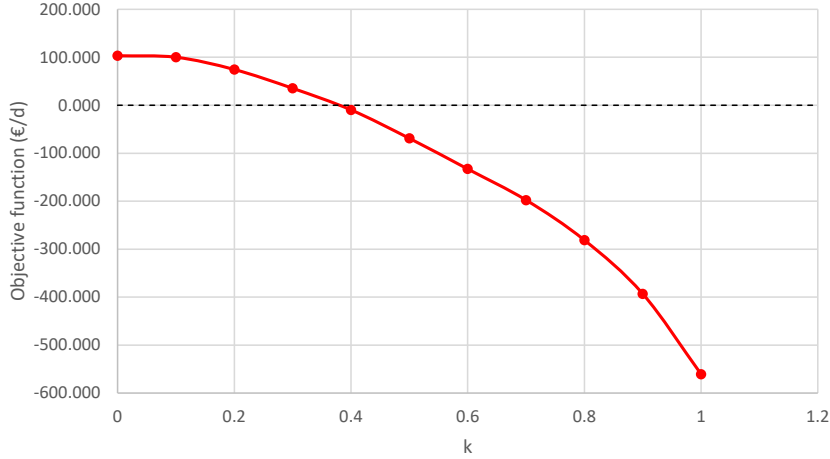


Figure 6.2: Sensitivity analysis on the parameter  $k$ .

As it was to be expected, the objective function decreases with the increase of  $k$  (displayed in Figure 6.2), because energy is sold at a higher price, thus reducing the costs. For values higher than  $k \approx 0.4$  the objective function becomes negative, due to earnings being higher than the costs, meaning that it is possible to turn a profit.

Moreover, it is evident how the slope of the curve is not always linear; in fact, it is possible to distinguish between three zones:

- $0 \leq k \leq 0.3$ : non-linear slope
- $0.4 \leq k \leq 0.7$ : linear slope
- $0.8 \leq k \leq 1$ : non-linear slope

This behavior can be explained by looking at the energy sold by the system (Figure 6.3): in the sections in which the slope is not linear, we can notice a significant increase in the amount of energy sold to the grid, while in the linear section this quantity remains more or less constant.

Furthermore, it is possible to observe how the sold thermal energy undergoes a much more dramatic increase than electric energy: this might be due to the fact that the thermal storage unit has a higher capacity than the electric one; moreover, the boiler has a thermal efficiency of 0.9: this means that in some cases we can turn a profit by simply buying natural gas and selling the thermal power produced.

## 6.3 Error due to linearization

To assess the efficacy of the efficiency curves linearization in different conditions, a cross sensitivity analysis on the parameters  $PH$  and  $k$  has been performed (Figures 6.4 and 6.5).

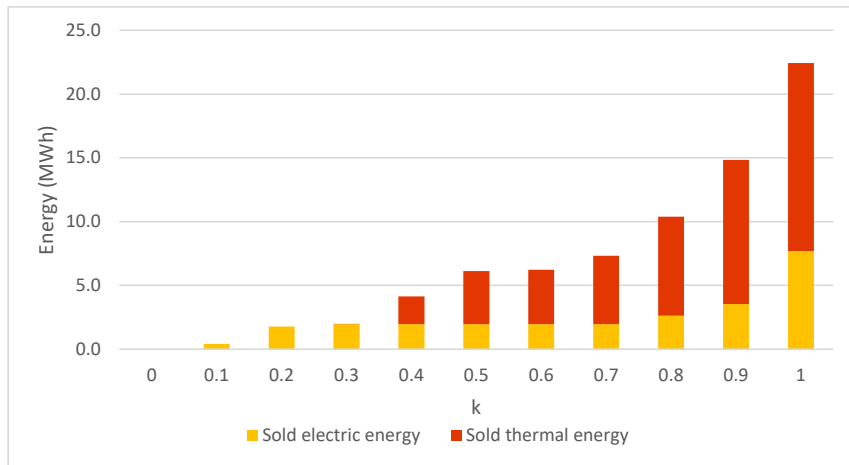


Figure 6.3: Energy sold for each value of the parameter  $k$ .

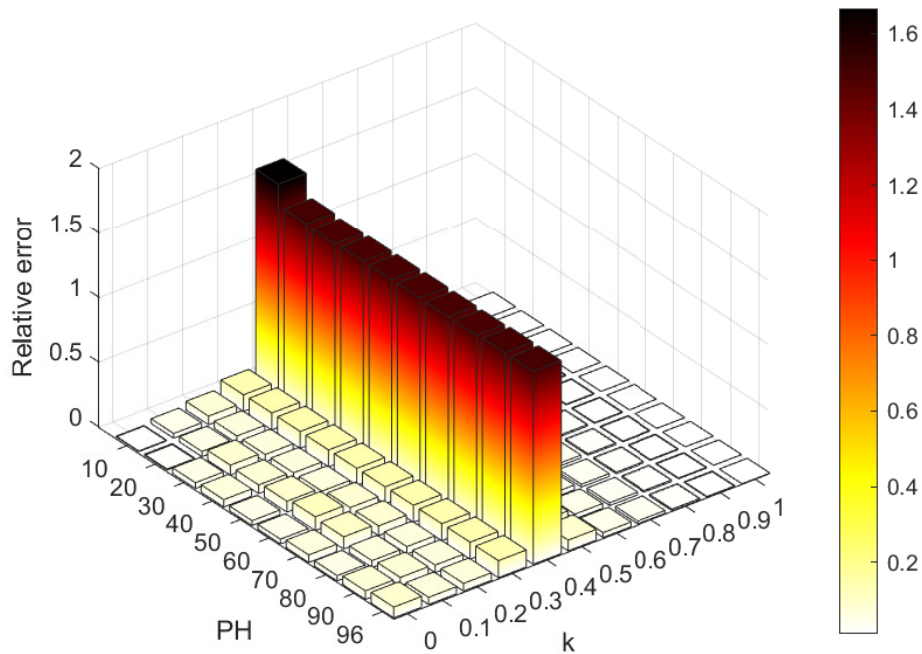


Figure 6.4: Relative error due to linearization.

By looking at Figure It is evident how the size of the prediction horizon doesn't have any noticeable effects on the relative error, while a dramatic spike is present for  $k = 0.4$ . This phenomenon can be explained by taking into account the absolute error values and comparing them to the objective function.

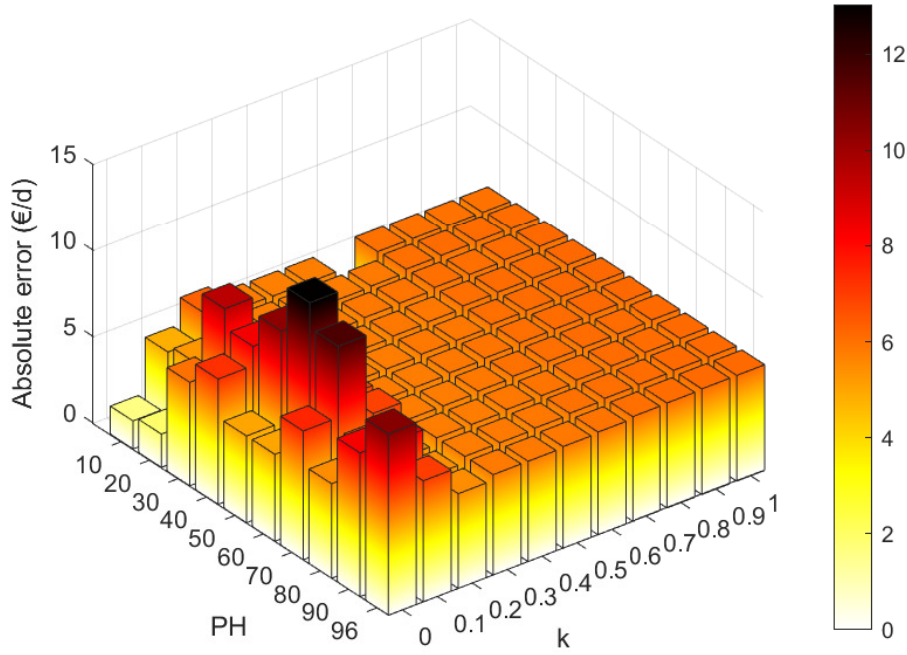


Figure 6.5: Absolute error due to linearization.

The absolute error remains almost constant with the varying of both  $PH$  and  $k$  (with the exception of a few cases for very low values of  $k$ ); the sudden spike in the relative error is due to the fact that for  $k = 0.4$  the objective function is very close to 0: in this case, the absolute error will weigh more in proportion to the total cost.

## 6.4 Uncertainty generation

For the previously presented results, the predicted energy demand has been subjected to a random uncertainty of  $\pm 20\%$ , with a uniform probability distribution. Nevertheless, one might want to also take into account the fact that uncertainty is higher for peaks in the demand; for this reason, two methods of uncertainty generation have been implemented:

- Constant uncertainty:** the actual energy demand is calculated as:  $\Phi_{i,actual}(t) = (1 - u) \cdot \Phi_i(t) + 2u \cdot \rho \cdot \Phi_i(t)$ , where  $u$  is the value associated to uncertainty (0.2 in this case) and  $\rho$  is a random value (generated with a uniform probability distribution) between 0 and 1.
- Uncertainty depending on peaks:** the actual energy demand is calculated as:  $\Phi_{i,actual}(t) = \Phi_i(t) + (-u + 2u \cdot \rho) \cdot (mean(\Phi_i) - \Phi_i(t))$ , where  $u$  is the value associated to uncertainty (1.5 in this case) and  $\rho$  is a random value (generated with a uniform probability distribution) between 0 and 1.

Here is a comparison between the two generation methods (Figures 6.6, 6.7 and 6.8):

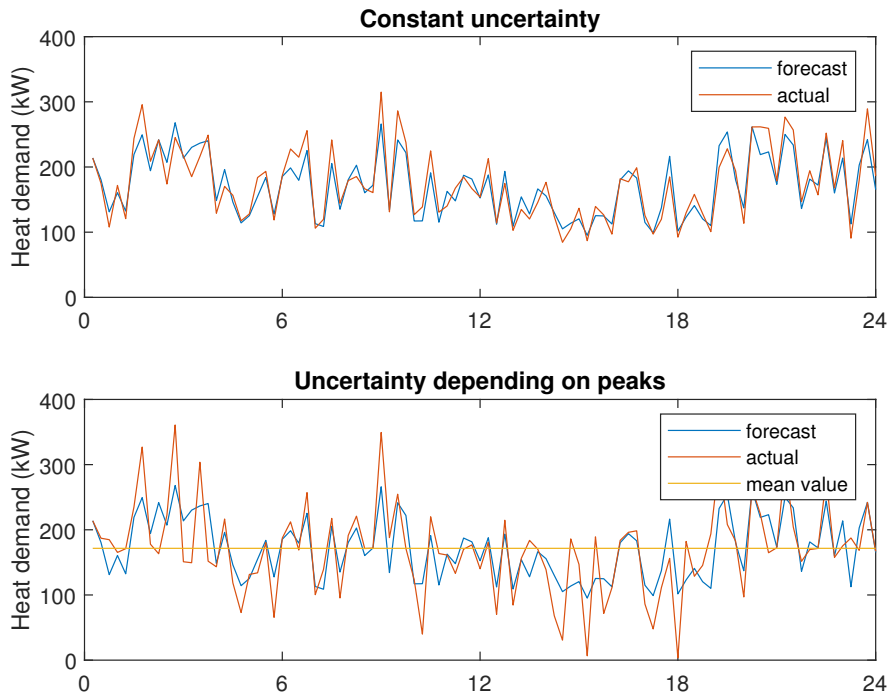


Figure 6.6: Uncertainty generation for heating demand.

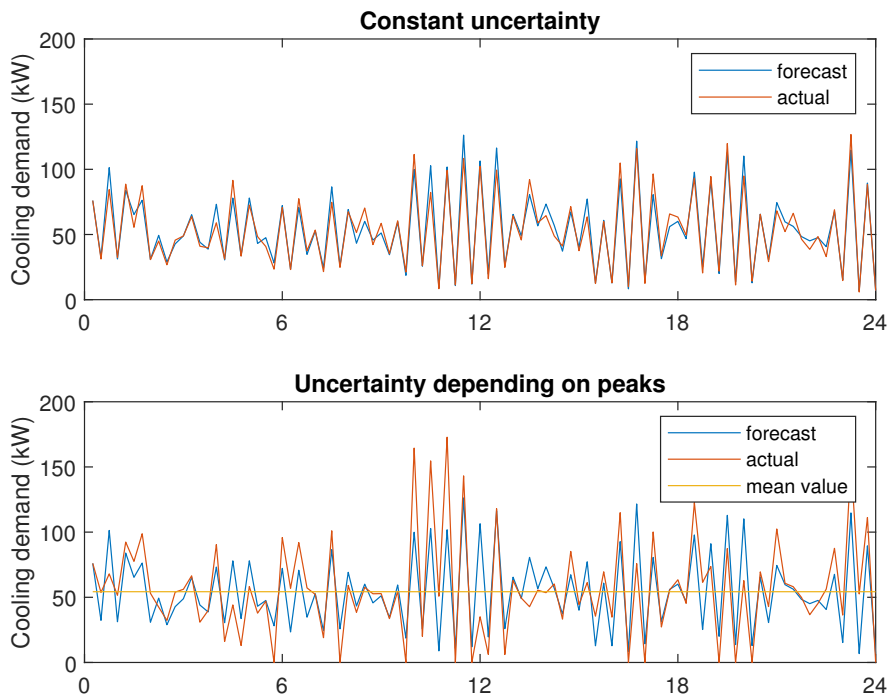


Figure 6.7: Uncertainty generation for cooling demand.

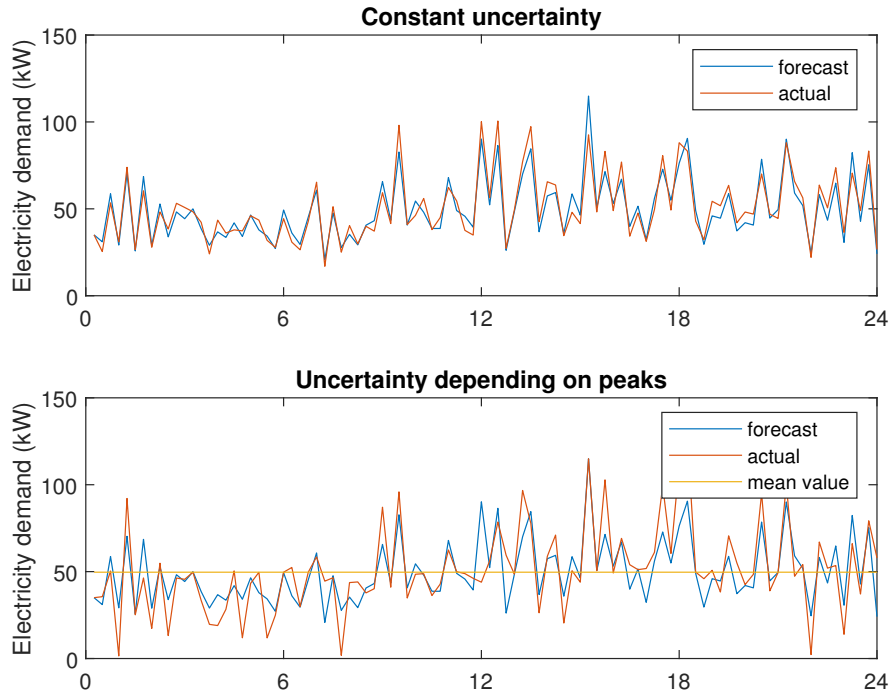


Figure 6.8: Uncertainty generation for electricity demand.

While the constant uncertainty generation method presents more or less a uniform variance with respect to the predicted energy needs, the second method concentrates it on the values which deviate more from the average demand.

After establishing the uncertainty generation methods, a cross sensitivity analysis on the value of  $u$  and  $PH$  was performed (Figures 6.9 and 6.10): both methods were applied, and each value of the objective function was then compared with the best possible solution (i.e. the objective function's value computed with no uncertainty and using a MILP optimization on the whole time window of the problem).

u	Difference wrt best solution										Best solution
	PH										
	10	20	30	40	50	60	70	80	90	96	
0	0.664	0.347	0.129	0.113	0.061	0.079	0.045	0.030	0.004	0.000	35.273
0.1	0.887	0.374	0.219	0.155	0.142	0.151	0.107	0.106	0.111	0.106	35.655
0.2	0.993	0.627	0.375	0.196	0.198	0.220	0.149	0.133	0.132	0.133	35.571
0.3	1.744	1.081	1.030	1.014	0.934	1.013	0.808	0.865	0.886	0.888	35.095
0.4	1.840	1.299	1.028	0.943	0.865	0.861	0.868	0.882	0.934	0.934	32.371
0.5	1.221	1.084	0.869	0.599	0.606	0.641	0.639	0.611	0.604	0.598	32.892
0.6	3.372	2.682	2.381	1.892	2.207	1.913	1.969	1.971	1.992	1.976	40.098
0.7	2.912	2.476	2.161	2.002	1.952	1.986	1.993	2.099	2.012	2.012	38.276
0.8	1.752	1.624	1.096	0.983	1.025	0.900	1.053	1.077	1.069	1.070	33.110
0.9	2.883	1.856	2.151	2.126	2.146	2.113	2.112	2.110	2.123	2.098	33.378
1	3.140	2.612	2.495	1.939	2.275	2.270	2.259	2.261	2.269	2.269	42.335

Figure 6.9: Sensitivity analysis for the constant uncertainty generation method.

u	Difference wrt best solution										Best solution
	PH										
	10	20	30	40	50	60	70	80	90	96	
0	0.664	0.347	0.129	0.113	0.061	0.079	0.045	0.030	0.004	0.000	35.273
0.25	0.833	0.277	0.135	0.100	0.092	0.083	0.050	0.018	0.032	0.000	35.216
0.5	1.233	1.043	0.927	0.846	0.854	0.830	0.818	0.812	0.816	0.815	35.545
0.75	0.959	0.602	0.503	0.437	0.406	0.396	0.400	0.379	0.409	0.351	35.322
1	1.247	0.902	0.513	0.382	0.431	0.368	0.410	0.392	0.422	0.414	32.967
1.5	1.227	0.712	0.653	0.623	0.606	0.512	0.684	0.557	0.653	0.606	31.087
2	1.111	0.919	0.623	0.573	0.442	0.324	0.349	0.343	0.336	0.337	34.724
2.5	3.192	2.810	2.490	2.180	2.175	2.201	2.198	2.238	2.240	2.240	38.188

Figure 6.10: Sensitivity analysis for the uncertainty depending on peaks generation method.

The overall trend is easily discernible (independently from the uncertainty generation method considered): the solution computed by the Rolling Horizon algorithm becomes "worse" (higher with respect to the optimal solution) when  $u$  increases (meaning that the forecast is less accurate and the optimization less efficient) and  $PH$  decreases (meaning that the algorithm has less degrees of freedom to compensate for the inaccurate prediction).

## 6.5 Imposed value of storage

In standard conditions, with no additional constraints, the algorithm will be inclined to impose the storage units' levels equal to 0 at the last time-step of the prediction horizon. This is because it would make no sense to store energy without using it, since this would involve additional costs. However, in real-life situations this might not always be the case: it could be useful to make sure that, at a certain time, the storage level is equal to a particular value.

A cross-sensitivity analysis has been performed on both the time and the level of the storage unit that have been imposed. The analysis was then performed for both uncertainty generation methods.

Additionally, a tolerance equal to 2% of the total capacity has been imposed on the storage levels, in order to allow the algorithm to manage both the additional constraints on the storage and the energy demand uncertainty (otherwise the simulation might stop because there is no feasible solution).

### 6.5.1 Imposed value on all three storage units

The storage level was imposed for all 3 storage units (Figures 6.11, 6.12 and 6.13).

Storage level	Time (h)								
	0.25	3	6	9	12	15	18	21	24
0%	37.379	37.151	38.798	37.798	37.632	36.847	38.471	36.989	36.907
10%	37.085	36.918	38.373	37.479	37.535	36.962	37.813	36.906	38.375
20%	39.485	36.830	38.014	37.325	37.370	37.284	37.596	36.853	40.434
30%	43.219	36.790	37.639	37.308	37.302	37.383	37.389	36.891	42.963
40%	48.004	36.954	37.373	37.149	37.240	37.727	37.169	37.030	45.199
50%	51.549	37.135	37.216	37.083	37.208	37.985	37.032	37.115	47.646
60%	56.705	37.332	37.116	37.040	37.195	38.142	37.098	37.464	50.178
70%	N.F.	38.111	37.213	37.022	37.206	38.439	37.059	37.829	52.806
80%	N.F.	39.096	37.508	37.077	37.229	38.750	37.167	38.195	55.456
90%	N.F.	41.561	37.806	37.083	37.254	39.093	37.369	38.567	58.120
100%	N.F.	43.959	38.132	37.233	37.458	39.553	37.592	38.949	60.819

Figure 6.11: Imposed level on 3 storage units: constant uncertainty

Storage level	Time (h)								
	0.25	3	6	9	12	15	18	21	24
0%	38.322	38.906	39.024	37.886	37.646	36.889	38.296	37.135	36.864
10%	37.196	36.942	38.407	37.549	37.539	36.949	37.950	36.988	38.381
20%	39.659	36.881	38.006	37.423	37.465	37.145	37.716	36.955	40.425
30%	43.399	36.992	37.682	37.320	37.404	37.355	37.497	36.919	42.753
40%	48.194	37.149	37.419	37.263	37.370	37.579	37.235	36.960	45.159
50%	51.668	37.297	37.200	37.254	37.340	37.817	37.089	37.228	47.606
60%	56.826	37.490	37.119	37.201	37.352	38.097	36.981	37.559	50.143
70%	N.F.	37.746	37.234	37.184	37.344	38.391	37.044	37.902	52.784
80%	N.F.	40.190	37.471	37.200	37.365	38.706	37.133	38.245	55.496
90%	N.F.	42.643	37.817	37.300	37.424	39.023	37.248	38.589	58.159
100%	N.F.	45.103	38.580	37.601	37.597	39.527	37.680	38.954	60.852

Figure 6.12: Imposed level on 3 storage units: uncertainty depending on peaks

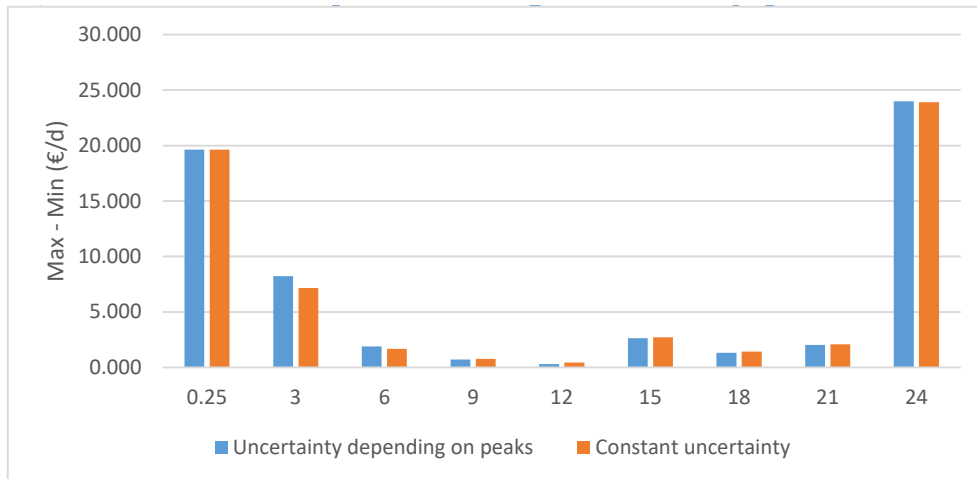


Figure 6.13: Difference between minimum and maximum objective function value.

It is possible to observe that imposing a storage level higher than 70% of the total capacity on the first time-step is not feasible; furthermore, the first and last time-step have the most severe effect on the objective function: in particular, imposing a high level of the storage on these time-steps will cause a dramatic increase in the total cost. On the other hand, the type of uncertainty generation holds almost no influence on the final result.

### 6.5.2 Imposed value on heat storage

The storage level was imposed for the heat storage unit (Figures 6.14, 6.15 and 6.16).

Storage level	Time (h)								
	0.25	3	6	9	12	15	18	21	24
0%	36.905	37.015	36.764	36.939	36.789	36.850	37.054	36.917	36.789
10%	36.802	36.856	36.789	36.790	36.798	36.805	36.913	36.850	37.300
20%	36.934	36.799	36.790	36.795	36.817	36.789	36.852	36.806	37.949
30%	37.596	36.811	36.871	36.814	36.841	36.844	36.801	36.792	38.602
40%	38.929	36.936	36.955	36.838	36.861	36.866	36.793	36.842	39.256
50%	40.265	37.103	37.072	36.863	36.911	36.886	36.814	36.905	39.915
60%	41.623	37.211	37.172	36.900	36.963	36.911	36.833	36.968	40.577
70%	42.992	37.389	37.309	36.948	37.025	36.955	36.863	37.035	41.243
80%	44.404	37.596	37.535	37.005	37.094	36.986	36.892	37.113	41.917
90%	45.799	37.790	37.700	37.073	37.183	37.055	36.933	37.193	42.624
100%	47.194	38.012	37.807	37.275	37.326	37.129	37.009	37.280	43.379

Figure 6.14: Imposed level on heat storage: constant uncertainty

Storage level	Time (h)								
	0.25	3	6	9	12	15	18	21	24
0%	37.854	37.131	36.948	37.029	36.846	36.905	37.141	37.015	36.843
10%	36.898	36.939	36.840	36.896	36.847	36.862	37.014	36.948	37.336
20%	37.117	36.843	36.843	36.893	36.910	36.849	36.935	36.903	37.951
30%	37.725	36.969	36.882	36.916	36.927	36.844	36.890	36.860	38.588
40%	39.062	37.065	36.917	36.934	36.935	36.853	36.863	36.846	39.226
50%	40.415	37.222	36.976	36.942	36.983	36.877	36.849	36.872	39.875
60%	41.781	37.403	37.113	36.988	37.035	36.908	36.845	36.899	40.533
70%	43.157	37.568	37.225	37.038	37.099	36.938	36.825	36.991	41.202
80%	44.533	37.770	37.381	37.095	37.165	36.971	36.847	37.040	41.909
90%	45.924	37.944	37.527	37.255	37.268	37.035	36.873	37.054	42.655
100%	47.319	38.159	37.648	37.500	37.377	37.111	36.936	37.132	43.431

Figure 6.15: Imposed level on heat storage: uncertainty depending on peaks

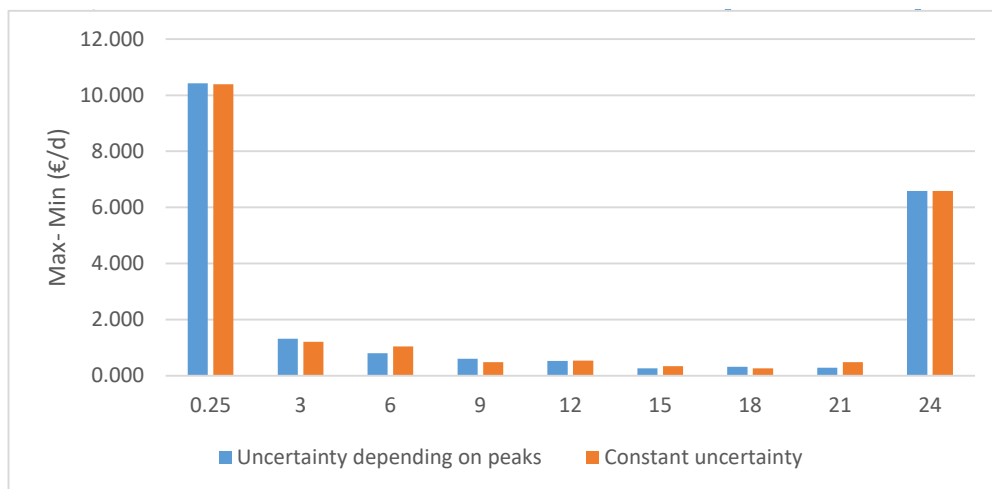


Figure 6.16: Difference between minimum and maximum objective function value.

In this case, there are no unfeasible solutions because it is possible to buy thermal energy from the grid; furthermore, the first and last time-step have the most severe effect on the objective function: in particular, imposing a high level of the storage on these time-steps will cause a dramatic increase in the total cost. On the other hand, the type of uncertainty generation holds almost no influence on the final result.

### 6.5.3 Imposed value on cool storage

The storage level was imposed for the cool storage unit(Figures 6.17, 6.18 and 6.19).

Storage level	Time (h)								
	0.25	3	6	9	12	15	18	21	24
0%	37.212	37.371	36.844	36.990	36.861	36.789	37.074	36.852	36.907
10%	36.789	36.854	36.852	36.845	36.812	36.813	36.789	36.851	36.986
20%	36.942	36.789	36.842	36.777	36.724	36.966	36.798	36.812	37.249
30%	37.371	36.733	36.702	36.816	36.721	36.882	36.817	36.865	37.698
40%	37.522	36.805	36.710	36.718	36.726	37.030	36.812	36.992	37.792
50%	37.665	36.758	36.742	36.713	36.745	37.086	36.882	37.038	38.075
60%	38.181	36.782	36.807	36.720	36.785	37.046	37.098	37.330	38.364
70%	N.F.	36.862	36.882	36.745	36.944	37.139	37.047	37.635	38.658
80%	N.F.	36.965	37.019	36.866	36.961	37.251	37.133	37.941	38.963
90%	N.F.	37.076	37.047	36.877	36.943	37.367	37.301	38.249	39.269
100%	N.F.	37.127	37.176	36.953	37.208	37.607	37.401	38.556	39.598

Figure 6.17: Imposed level on cool storage: constant uncertainty

Storage level	Time (h)								
	0.25	3	6	9	12	15	18	21	24
0%	38.155	38.015	37.076	37.070	36.875	36.818	36.898	36.968	36.864
10%	36.884	36.898	36.869	36.910	36.843	36.824	36.819	36.868	37.017
20%	37.045	36.850	36.822	36.878	36.828	36.858	36.828	36.888	37.273
30%	37.366	36.843	36.826	36.830	36.822	36.890	36.847	36.867	37.525
40%	37.578	36.831	36.861	36.825	36.869	36.925	36.807	36.923	37.808
50%	37.713	36.857	36.883	36.867	36.867	36.987	36.877	37.186	38.106
60%	38.223	36.905	36.897	36.842	36.914	37.045	36.950	37.480	38.410
70%	N.F.	36.990	36.970	36.867	36.932	37.102	37.033	37.786	38.720
80%	N.F.	37.041	37.052	36.937	36.987	37.194	37.126	38.092	39.031
90%	N.F.	37.138	37.224	36.984	37.067	37.291	37.227	38.399	39.364
100%	N.F.	37.244	37.338	37.111	37.242	37.534	37.491	38.707	39.656

Figure 6.18: Imposed level on cool storage: uncertainty depending on peaks

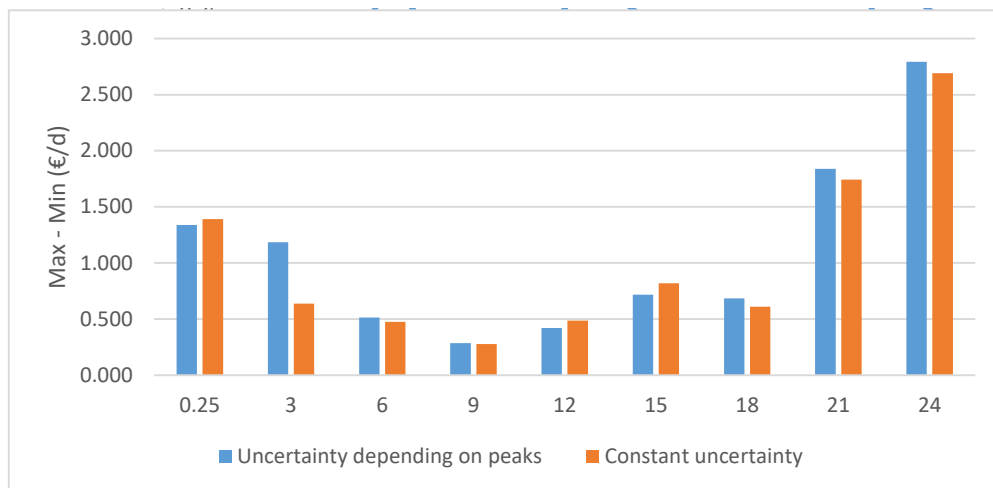


Figure 6.19: Difference between minimum and maximum objective function value.

It is possible to observe that imposing a storage level higher than 70% of the total capacity on the first time-step is not feasible; in this case, the first and last time-steps still are the most influential on the final solution, but the difference between the maximum and minimum values of the objective function is much smaller than in the other cases. Except for the 3rd hour, there is no significant difference between the two uncertainty generation types.

### 6.5.4 Imposed value on electric storage

The storage level has been imposed for the electric storage unit (Figures 6.20, 6.21 and 6.22).

Storage level	Time (h)								
	0.25	3	6	9	12	15	18	21	24
0%	37.071	36.828	38.748	37.556	37.560	36.789	37.881	36.822	36.789
10%	37.073	36.793	38.311	37.424	37.482	36.910	37.693	36.791	37.653
20%	39.301	36.820	37.961	37.324	37.403	37.131	37.505	36.794	38.835
30%	41.529	36.847	37.634	37.247	37.324	37.286	37.316	36.805	40.289
40%	43.758	36.874	37.317	37.171	37.246	37.477	37.128	36.816	41.786
50%	45.986	36.901	37.031	37.094	37.167	37.668	36.940	36.827	43.311
60%	48.214	36.927	36.797	37.018	37.088	37.858	36.789	36.838	44.916
70%	50.442	36.994	36.791	36.941	37.010	38.049	36.789	36.848	46.606
80%	52.670	38.248	36.889	36.864	36.931	38.240	36.796	36.859	48.307
90%	54.899	40.497	37.054	36.789	36.852	38.431	36.811	36.870	50.007
100%	57.127	42.745	37.237	36.803	36.789	38.621	36.896	36.881	51.708

Figure 6.20: Imposed level on electric storage: constant uncertainty

Storage level	Time (h)								
	0.25	3	6	9	12	15	18	21	24
0%	38.021	36.882	38.769	37.601	37.614	36.843	37.976	36.880	36.843
10%	37.127	36.847	38.377	37.470	37.536	36.945	37.788	36.848	37.715
20%	39.355	36.874	38.023	37.378	37.457	37.099	37.600	36.846	38.906
30%	41.583	36.901	37.696	37.301	37.378	37.289	37.412	36.857	40.371
40%	43.812	36.928	37.388	37.225	37.300	37.480	37.223	36.867	41.880
50%	46.040	36.955	37.102	37.148	37.221	37.671	37.035	36.878	43.406
60%	48.268	36.992	36.867	37.072	37.142	37.862	36.869	36.889	45.009
70%	50.496	37.063	36.846	36.995	37.064	38.052	36.843	36.900	46.699
80%	52.724	39.295	36.960	36.919	36.985	38.243	36.854	36.911	48.392
90%	54.953	41.543	37.128	36.843	36.906	38.434	36.868	36.921	50.092
100%	57.181	43.791	37.310	36.857	36.843	38.624	36.985	36.932	51.793

Figure 6.21: Imposed level on electric storage: uncertainty depending on peaks

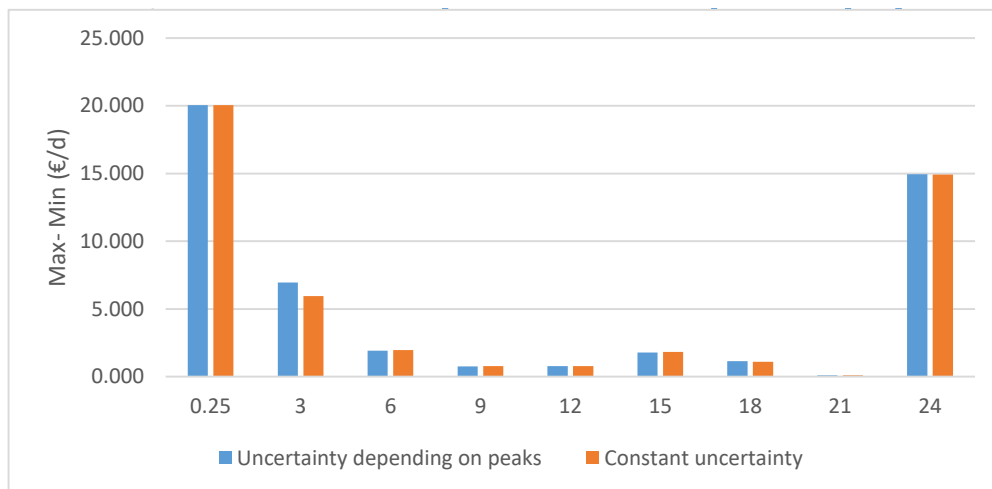
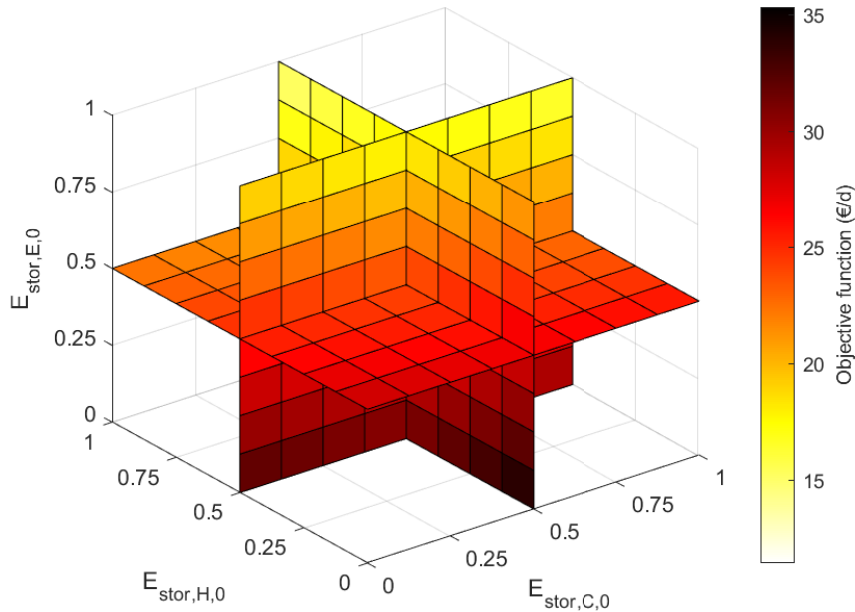


Figure 6.22: Difference between minimum and maximum objective function value.

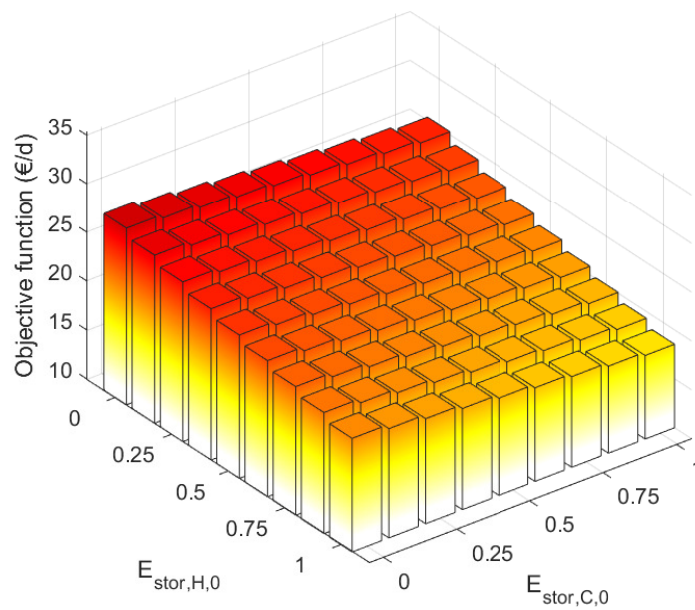
In this case, there are no unfeasible solutions because it is possible to buy electric energy from the grid; furthermore, the first and last time-step have the most severe effect on the objective function: in particular, imposing a high level of the storage on these time-steps will cause a dramatic increase in the total cost. On the other hand, the type of uncertainty generation holds almost no influence on the final result.

## 6.6 Initial level of storage

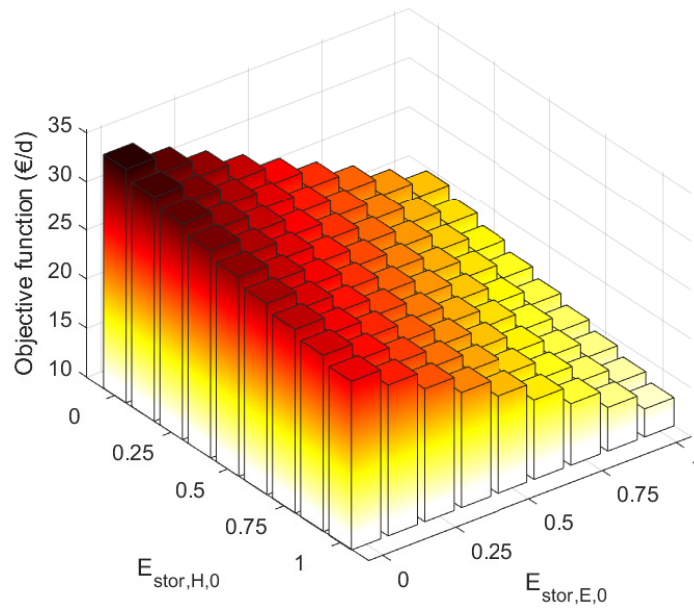
All of the analyses so far have been performed by supposing that, at the beginning of the simulated day, all of the storage units are empty. It is possible to perform a sensitivity analysis on this parameter, too, which will be useful to see which type of storage influences the objective function's value the most (Figure 6.23).



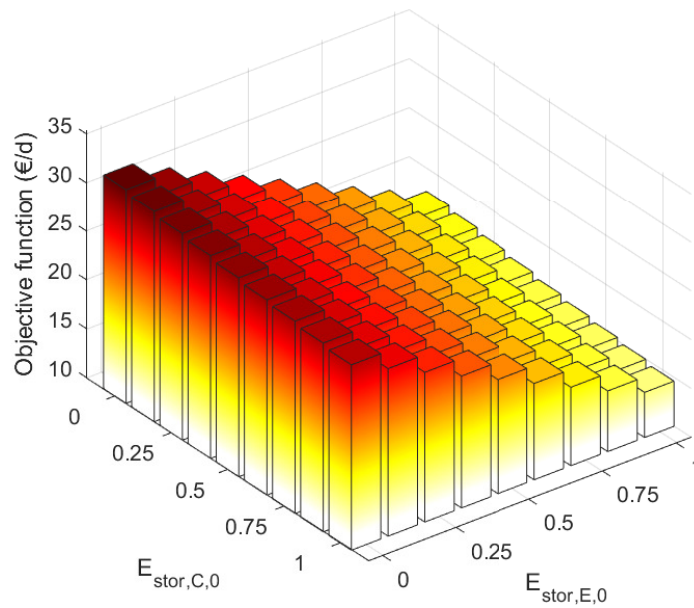
(a) 3D visualization of the objective function's sensitivity to the storage level. The planes correspond to 50% of the total capacity.



(b) Sensitivity to heat and cooling storage. Electric storage level is equal to 50% of the total capacity.



(c) Sensitivity to heat and electric storage. Cooling storage level is equal to 50% of the total capacity.



(d) Sensitivity to cooling and electric storage. Heat storage level is equal to 50% of the total capacity.

Figure 6.23: Sensitivity of the objective function to the storage's initial level.

It is possible to see that the type of storage which has the greatest influence on the objective function is the electric one, closely followed by the heat storage; on the other hand, the cooling storage has a much smaller impact on the total cost: this is probably because cooling thermal power is the only one which cannot be sold to the grid. Furthermore electric power is a more "valuable" type of energy than heat, since it has a higher production cost and a higher market price.



# Chapter 7

## Conclusions

The purpose of the thesis was to increase the overall efficiency of the operation of a complex energy system, in order to satisfy the given energy demands and to minimize monetary expenses. A suitable optimization algorithm, named "Rolling Horizon", was chosen and implemented in order to achieve this result.

After a brief introduction on Hybrid Renewable Energy Systems and optimization algorithms, the problem to solve was analyzed: the starting data were introduced and each component was concisely described. Afterwards, the Rolling Horizon method was presented and explained via a step-by-step walk-through. Subsequently, the available data were manipulated in order to employ them in the linear optimization algorithm: the efficiency curves were approximated with a linear fit and the optimization problem was formulated.

Following the first iteration of the linear optimization algorithm, several issues arose, such as: the zero-degree efficiency term leading to inaccurate results, the impossibility of imposing a minimum power value different from 0 without having a component always turned on, the inaccurate linear approximation of the electric chiller and the gas heat pump. To be able to overcome these problems, the standard linear programming optimization was substituted with a Mixed Integer Linear Programming approach, which requires more computational effort but is better suited for the formulation of this problem; using this method the algorithm gained the ability to discern between ON and OFF states of components and the possibility to apply a three-piece linear fit to the electric chiller's efficiency and a two-piece linear fit to the gas heat pump's cooling efficiency (which led to a much more accurate approximation of the curve).

After completing the formulation of the Mixed Integer Linear Programming optimizer, it was possible to apply it within the Rolling Horizon algorithm: for the initial simulation, the values of the parameters  $k$  (corresponding to the ratio between the selling and buying price of thermal and electric energy) and  $PH$  (the size of the prediction horizon) were chosen hypothesizing a realistic scenario in which this method would be applied. To assess the actual efficacy of the algorithm, the results were compared with a "priority order" operation method, in which an order was assigned to the activation of the system's components: the most efficient ones are the first ones to be employed, then the other ones are activated in sequence (according to their efficiency); in this case there is no forecast on the future demand, which explains why the storage units are never used. The objective function's value obtained with this method is €124.72, 253% higher than the Rolling Horizon opti-

mization's result. A further comparison was made with a standard Mixed Integer Linear Programming optimization (computed at the beginning of the day on the whole time window of the problem), in which no adjustments are made during the operation of the system to account for the uncertainty in the forecast; this method also performed very poorly when compared to the Rolling Horizon simulation (€77.33 daily cost, for a 119% increase in the objective function). Afterwards, the error due to the linearization of the problem was computed, and it was deemed acceptable in comparison to the previous simulations (around €6 per day).

In the final part of the work, a sensitivity analysis was performed on the most relevant parameters of the algorithm: it was found that  $k$  (ratio between selling and buying price of energy) greatly influences the system's behavior and the value of the objective function (which decreases with the increase of  $k$ ); the size of the Prediction Horizon  $PH$  affects the computed solution's efficacy, but for large values the decrease in the objective function becomes negligible and increasing  $PH$  only leads to a negative effect on the computational effort. The absolute error due to the linearization of the problem is not affected by neither of the previously mentioned parameters, while the relative error depends on the value of the objective function. Furthermore, the uncertainty's severity also affects the solution: the results show that the algorithm computes a worse solution when uncertainty increases, showing that the forecast needs to be as accurate as possible. A further analysis was made on the effect of the storage units level on the solution: it was found that the objective function is most sensitive to the electric storage level, followed by the heat storage and the cool storage.

In conclusion, the Rolling Horizon algorithm proved to be a flexible and reliable method to manage a complex energy system, especially in scenarios characterized by great uncertainty. Moreover, if the Prediction Horizon is chosen carefully it can significantly decrease the computational effort without much reducing the solution's accuracy.



# List of Symbols

## *Notation*

<b>Symbol</b>	<b>Meaning</b>	<b>Unit</b>
$t$	Time	s
$t_0$	Time of the current iteration	s
$\Delta t$	Time-step duration	s
$PH$	Prediction Horizon	-
$CH$	Control horizon	-
$c'$	Costs vector	-
$c$	Energy price	€/kWh
$x$	Control variables vector	-
$A$	Inequality constraints coefficients matrix	-
$b$	Inequality constraints known terms vector	-
$A_{eq}$	Equality constraints coefficients matrix	-
$b_{eq}$	Equality constraints known terms vector	-
$\Phi$	Power	kW
$E$	Energy	kWh
$T$	Temperature	°C
$T_0$	Reference temperature	°C
$v$	Wind Speed	m/s
$u$	Uncertainty parameter	-
$\eta$	Efficiency	-
$Y$	Binary variable	-

## *Superscripts and subscripts*

<b>Symbol</b>	<b>Meaning</b>
<i>i</i>	i-th unit
<i>j</i>	j-th unit
<i>H</i>	Heating
<i>C</i>	Cooling
<i>E</i>	Electricity
<i>G</i>	Natural gas
<i>CHP</i>	Combined Heat and Power unit
<i>GHP</i>	Geothermal Heat Pump
<i>Boil</i>	Boiler
<i>Abs</i>	Absorption chiller
<i>Chill</i>	Electric chiller
<i>Stor</i>	Storage
<i>PV</i>	Photovoltaic panel
<i>env</i>	Environment
<i>IN</i>	Inlet
<i>OUT</i>	Outlet

# Bibliography

- a.s., TEDOM. URL: <https://www.tedom.com>.
- centre, Efficient energy. URL: <http://www.efficientenergycentre.co.uk/heat-pumps/>.
- Cryan, Paul. URL: <https://www.usgs.gov/media/images/wind-turbine-and-forest>.
- Electric, General. URL: <https://www.ge.com/reports/leading-charge-battery-storage-sweeps-world-ge-finding-place-sun/>.
- IEA. *World Energy Outlook 2019*. 2019.
- LG. URL: <https://www.lg.com/us/business/solar-panels/lg-lg340n1c-v5#>.
- Nunes, Giovani Cavalcanti. *Design and analysis of multivariable predictive control applied to an oil-water-gas separator: a polynomial approach*. 2001. URL: <http://citeseerx.ist.psu.edu/viewdoc/download?doi=10.1.1.6.6300&rep=rep1&type=pdf>.
- Piho, Markki. URL: <http://www.markki.com/design/thermal-energy-storage-tanks/>.
- Products, Thermotech Green. URL: <http://thermotechgp.com/absorption-chiller/>.
- Saharia, Barnam. "A review of algorithms for control and optimization for energy management of hybrid renewable energy systems". In: *Journal of Renewable and Sustainable Energy* (2018).
- Systems, Engineered. URL: <https://www.esmagazine.com/articles/98678-york-yz-magnetic-bearing-centrifugal-chiller-johnson-controls>.
- Viessmann. URL: <https://www.viessmann.it/it/riscaldamento-casa/caldaie-a-condensazione-a-gas/caldaie-a-condensazione-a-gas-murali/caldaia-condensazione-vitodens-200w.html>.